REPUBLIC OF TÜRKİYE

ALTINBAŞ UNIVERSITY

Institute of Graduate Studies

Mechanical Engineering

IMPROVING THERMAL EFFICIENCY OF PHOTOVOLTAIC THERMAL SYSTEMS

Mohammed Abbas Fadhil AL-KHAFAJI

Master's Thesis

Supervisor

Asst. Prof. Dr. İbrahim KOÇ

Istanbul, 2023

IMPROVING THERMAL EFFICIENCY OF PHOTOVOLTAIC THERMAL SYSTEMS

Mohammed Abbas Fadhil AL-KHAFAJI

Mechanical Engineering

Master's Thesis

ALTINBAŞ UNIVERSITY

2023

The thesis titled “IMPROVING THERMAL EFFICIENCY OF PHOTOVOLTAIC THERMAL SYSTEMS” prepared and presented by MOHAMMED ABBAS FADHIL AL-KHAFAJI and submitted on 14/ 4 /2023 has been accepted unanimously for the degree of Master of Science in Mechanical Engineering.

Asst. Prof. Dr. İbrahim KOÇ

Supervisor

Thesis Defense Jury Members:

Asst. Prof. Dr. İbrahim KOÇ.	Department of Mechanical Engineering, Altınbaş University	_____
Asst. Prof. Dr. Serday AY	Department of Mechanical Engineering, Altınbaş University	_____
Asst. Prof. Dr. Haydr UYANIKU	Department of Mechanical Engineering, Karatay University	_____

I hereby declare that this thesis meets all format and submission requirements of a Master’s thesis.

Submission date of the thesis to Institute of Graduate Studies: ___/___/___

I hereby declare that all information in this document has been obtained and presented in accordance with academic rules and ethical conduct. I also declare that, as required by these rules and conduct, I have fully cited and referenced all material and results that are not original to this work.

Mohammed Abbas Fadhil AL-KHAFAJI

Signature

DEDICATION

I am dedicating this thesis to beloved people who have meant and continue to mean so much to me. First and foremost, to my parents whose love for me knew no bounds and, who taught me the value of hard work. My sisters Zahraa and Farah have never left my side and are very special, they encouraged me to pursue my dreams and finish my dissertation.

PREFACE

I would like to extend my sincere thanks to Asst. Prof. Dr. İbrahim KOÇ, lecturer at Altınbaş University, Department of Mechanical Engineering, who was my supervisor during the writing of this research and who gave me the right direction by providing much correct advice, instructions, and information. Would also like to thank Assoc. Prof. Dr. Süleyman BAŞTÜRK, Head of the Mechanical Engineering Department at Altınbaş University, who in turn assisted immediately to solve all technical problems from laboratories and others. Also thanks to all the friends who supported, encouraged me and gave me valuable advice and information.

ABSTRACT

IMPROVING THERMAL EFFICIENCY OF PHOTOVOLTAIC THERMAL SYSTEMS

AL-KHAFAJI, Mohammed Abbas

M.Sc., Mechanical Engineering, Altınbaş University,

Supervisor: Asst. Prof. Dr. İbrahim KOÇ

Date: April / 2023

Pages: 74

Photovoltaic panels can convert solar energy directly into electricity, but their efficiency declines as the panels' temperature rise. To solve this problem, Photovoltaic thermal (PVT) systems have been developed to enhance power energy generation from Photovoltaic panels. This research presents the daily and monthly global solar radiation on a horizontal surface in Iraq and applies it to the PVT water system. The thesis contributes in two ways: first, it models a novel copper pipe system that improves thermal efficiency in an actual environment, and second, it investigates the hourly and daily intensity of solar radiation in Iraq. Using collected irradiation at mass flow rates ranging from 0.01 and to 0.02 kg per second, the surface temperature of the PVT model was calculated. Using the experimental data, the surface temperature was also computed in the PVT model. The findings were essentially consistent with those of prior investigations. A PVT system with a constant input temperature is employed to raise the surface temperature throughout simulated testing. This research considers the four unique seasons' weather conditions. With an optimal mass flow rate of 0.02 kg/s and a constant low input temperature, the findings demonstrate the thermal efficiency of the PVT.

Keywords: PVT, Water Flow, Thermal Efficiency, Power-Volt Curve, Alternating Current.

TABLE OF CONTENTS

Pages

LIST OF TABLES

Pages

LIST OF FIGURES

Pages

ABBREVIATIONS

L/D	:	The Screw's Flighted Length to Outer Diameter Ratio
PVT	:	Photovoltaic Thermal
Si cells	:	Crystalline Silicon Cell
mV	:	Volts to Millivolts
mA	:	Milliampere Electric Current
I-V	:	Current-Volt Curve
P-V	:	Power-Volt Curve
AC	:	Alternating Current
PCM	:	Phase Change Material
A	:	Ampere
V	:	Voltage
kg	:	Kilogram
R	:	Radius of the Hole
DC	:	Direct Current

LIST OF SYMBOLS

μ	:	Viscosity
H	:	Channel Depth
τ	:	Shear rate in the Round Channel
Q	:	Volumetric Flow Rate
K	:	Resistance Factor
L	:	Channel Length
ΔP	:	Pressure Drops Across the Channel
ε	:	Shear Stress
F	:	Force Applied
A	:	Area
C	:	Heat Capacity
C_p	:	Specific Heat at Constant Pressure
ρ	:	Density
T	:	Temperature
η	:	Efficiency
I	:	Current
P	:	Power

1. INTRODUCTION

1.1 OVERVIEW

Solar energy may be created by several inventive techniques, including the capture of solar light and heat. These approaches include molten salt power plants, solar architecture, solar heating, photovoltaics, artificial photosynthesis, solar thermal energy, and among others. Light and heat emitted by the Sun are examples of what is known as solar energy. Significant volumes of clean energy are produced as a result of this procedure. Depending on whether they actively collect and distribute solar energy or convert solar light into electricity, their approaches are frequently classified as either active or passive solar, with the active category being more prevalent. The fundamental classification criterion is the method by which these devices transform solar energy. Using photovoltaic cells, concentrated solar power plants, and solar water heaters, active solar technology collects energy from solar beams [1].

Examples of passive solar architecture include positioning a building to face the Sun, employing materials with a high thermal mass or that scatter light well, and incorporating ventilation gaps. Because solar energy is abundant, it is an attractive alternative for use as a renewable energy source [2]. The International Energy Agency concluded in 2011 that there would be significant long-term benefits to developing technology for cheap, inexhaustible, environmentally friendly solar energy. Using solar energy keeps the price of fossil fuels low while also fostering sustainability, reducing pollution, and lowering the cost of solving global warming. In addition to bolstering national energy security, switching to a domestic, limitless, and import-free source has other benefits. Such benefits frequently occur.

Therefore, the initial deployment fees should be viewed as investments in learning, and used wisely and completely. Solar light is a renewable energy source because it may be collected indefinitely. The use of solar energy in the production of electricity has the added benefit of lowering the nation's reliance on imported fossil fuels, which is especially helpful for countries that have a hard time meeting their own electrical energy processing needs. Solar energy also has the potential to be used to heat water for domestic usage. Solar energy is a practical means of producing electricity in places where it is not otherwise available. Maintaining a solar system doesn't need much time or effort. The vast majority of solar panel

producers now guarantee their wares for 20–25 years, which means they last longer and cost less. In addition, solar energy can be used in many different ways that contribute to and improve our economy, society, and environment. [4].

The photovoltaic component of this system provides the majority of the available heat. The photovoltaic effect is the process through which semiconducting materials transform light into electricity. Silicon is utilized because it can conduct electricity. This essential component undergoes the incorporation of contaminants [5] such as boron and phosphorus. When Solar light strikes a photovoltaic panel, the presence of these contaminants creates the required circumstances for electron release. The generation of electricity eventually occurs from the release of electrons.

The adoption of solar photovoltaic (PV) cells has been hindered by high production costs, a lack of readily available components, and toxicity. Ended 2016 with a global installed capacity of around 300 gigawatts, it is expanding rapidly. Solar photovoltaic is utilized in over a hundred countries. China's market is now expanding the fastest, followed by Japan and the United States. In terms of installed capacity, photovoltaic is currently the third most significant renewable energy source [6] in the world. Consequently, current research has provided light on the operational aspects of photovoltaic. In this study, photovoltaics were researched and discussed to determine the operational variables and qualities that guide the researchers' efforts to develop and improve this system.

1.2 SOLAR PHOTOVOLTAIC SYSTEM (PV)

Solar photovoltaic systems include the use of micro inverters as opposed to a central inverter, the use of crystalline silicon as opposed to thin-film technology, and the use of modules made by Chinese manufacturers as opposed to those made by European and American manufacturers. The solar array plus a variety of other components, which are together referred to as the balance of the system, make up the photovoltaic system that supplies the energy needed for a residential, commercial, or industrial building. The balance of the system consists of the solar array, the mounting, the wiring, the tracker, the inverter, the battery, and the monitoring and metering. In addition to the optical lenses or mirrors, the system also requires a cooling system, as shown in Figure 1.1 [7].

Solar collector performance can be enhanced by transforming it into a double-pass collector, as demonstrated by Goh Li Jin [8]. A double-pass photovoltaic thermal solar collector was developed and tested during Sopian's [6] tenure on the project. The research found that an increase in the heat transfer coefficient due to turbulence enhances the overall performance of the system.

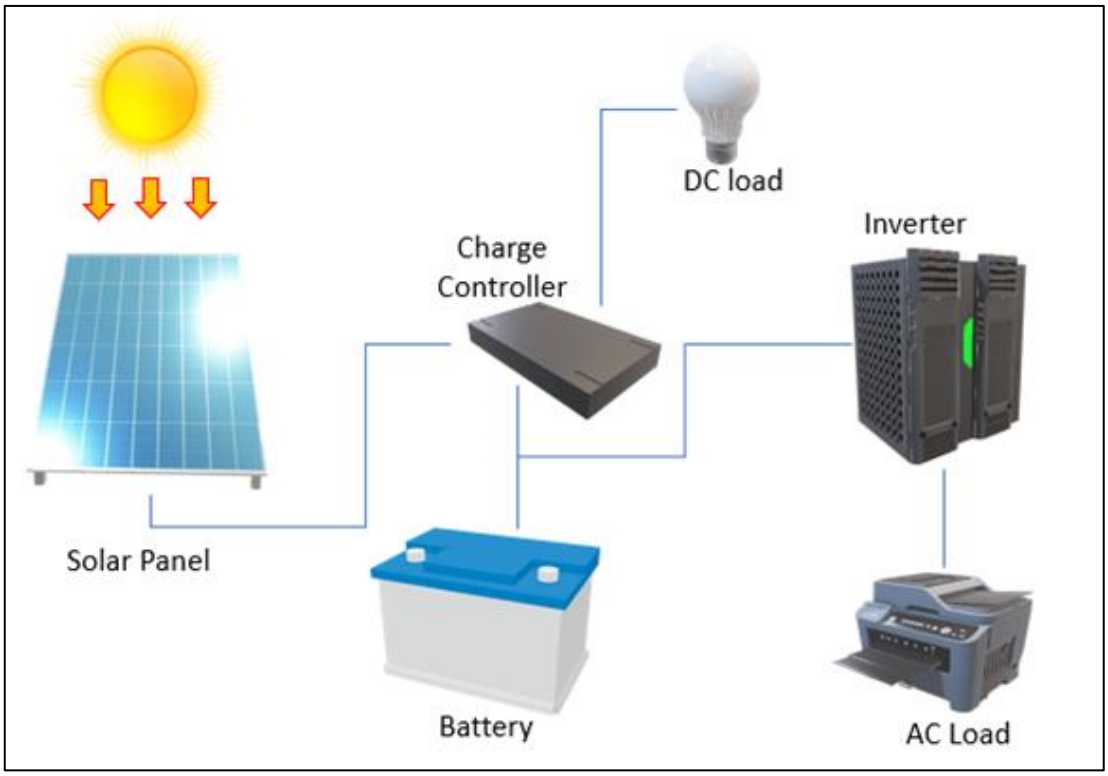

Figure 1.1: Components of a Photovoltaic System [7].

Othman [9], the designer of a double-pass photovoltaic-thermal solar air heater, came up with the idea. In this particular setup, the fins are inserted into the second channel flow passage in a direction that is perpendicular to the length of the collector. The photovoltaic panel's efficiency is improved as a result of the fins that are attached to its back. These fins facilitate the transmission of heat from the panel to the surrounding air. The double-pass photovoltaic/thermal solar air collector equipped with fins and a compound parabolic concentrator generates an excellent amount of electrical and thermal energy [10].

1.3 PROBLEM STATEMENT

Because of the high temperatures in Iraq, there has been a spike in the demand for PVT systems, which has led to an increase in the country's overall usage of power. In addition, Iraq is plagued by an insufficient supply of electrical energy; more specifically, during the last thirty years, Iraq's supply of electrical energy has decreased by fifty percent. This study makes the presumption that this issue might be resolved by employing alternative strategies for the generation of electrical energy by relying on sources of energy that are renewable, favorable to the environment, and cost-effective.

This may help solve the problem, as well as enhance the total amount of time that electricity is available. The low energy conversion efficiency of photovoltaic cells presents a significant challenge for solar photovoltaic (PV) systems. When the temp of the PV cells is allowed to rise above a particular threshold, there is a considerable drop in the cells' overall efficiency. It is important to bring the array's operating temp down to a lower setting to achieve the desired gain in efficiency. The difficulty lies in determining whether or not new research offers the optimum solutions for the generated heat effect caused by heat transfer growth based on the structural component design of solar systems.

1.4 STUDY OBJECTIVES

The objective of the present study is to analyze the cooling system geometry of photovoltaics based on different shapes regarding to water flow velocity and type. It can be specified in the following:

a. To build an effective model which involves specific sectional areas for the PVT system.
b. To investigate different conditions of cooling systems.

1.5 THE AIM OF STUDY

The research aims to improve the performance of the solar cell through the water cooling process. The process is carried out by passing the water through tubes of copper in a different way, as the shape of the tube path and the speed of the water are among the most important factors that help improve the cooling process of solar cells. To discover this process, there are several practical stages. The first stage is to discover the intensity of solar radiation in

Iraq, depending on specific times of the moon. The second stage is to test the effect of the intensity of solar radiation on the temperature of the solar cell, and then cool the solar panel with water through a set of tubes using different speeds.

1.6 THESIS STRUCTURE

The structure of the thesis was separated into five chapters.

Chapter 1 presents a general introduction to this study and discusses the state of the art of related studies, then present the problem statement, objectives aim of the study, and thesis organization.

Chapter 2 presents a review of the related studies developed to discuss and find the methods and functions related to photovoltaic systems and components.

Chapter 3 presents the thesis methodology used in the experiments and simulation processes.

Chapter 4 involves the results gained from the simulation run using experiments.

In chapter 5, conclusions and scope for future work have been stated finally.

2. LITERATURE REVIEW

2.1 INTRODUCTION

To transport heat from the solar into another medium, solar collectors employ the solar's kinetic energy. An essential part of every solar-powered setup is the solar collector. It is an apparatus that absorbs the sun's rays, converts them into heat, and then transfers that heat to the fluid passing through it (normally oil, air, and water). The collected solar energy is either utilized immediately to heat water, transferred to an air conditioner, or stored in a thermal energy depot for use throughout the night or on cloudy days. The two main categories of solar collectors on the market today are condensing and non-condensing models.

Also, the retention and extraction of thermal energy from chemical processes necessitate opposite reactions. Sensible heat storage usually requires a bigger vessel and more processing power because it relies on the bulk output of the substance, the specific heat, and the heat transition. The implementation of phase change material (PCM), one of the alternative thermal control methods, was investigated by Ali et al. In 2021 with the potential to lower cell temperature. To overcome a broad temp, range and lower the temp of the PV panel, three different kinds of PCM are combined in the suggested system. The use of phase-changing materials can control the temp of PV panels to a particular range, according to quantitative modeling and simulation. A benefit of PV panel regulation within a particular temp range was offered by the PCM materials. By similarly using the PCM to regulate temp, the solar panel voltage and maximum power MMP are also impacted. The contrast demonstrates that our suggested approach significantly reduces temp [11].

Rotating condenser collectors, hence increase the flux of radiation, whereas the non-condensing collectors' area to receive solar radiation is equal to their absorption area. When working with extreme heat, condensate collectors perform admirably. Whether the solar collectors are enclosed or open, and what fluids are utilized for heat transmission (air, antifreeze, water, or heat transfer oils) are all ways to classify the devices. Figure 2.1 demonstrates that there is a large supply of them on the market right now [12].

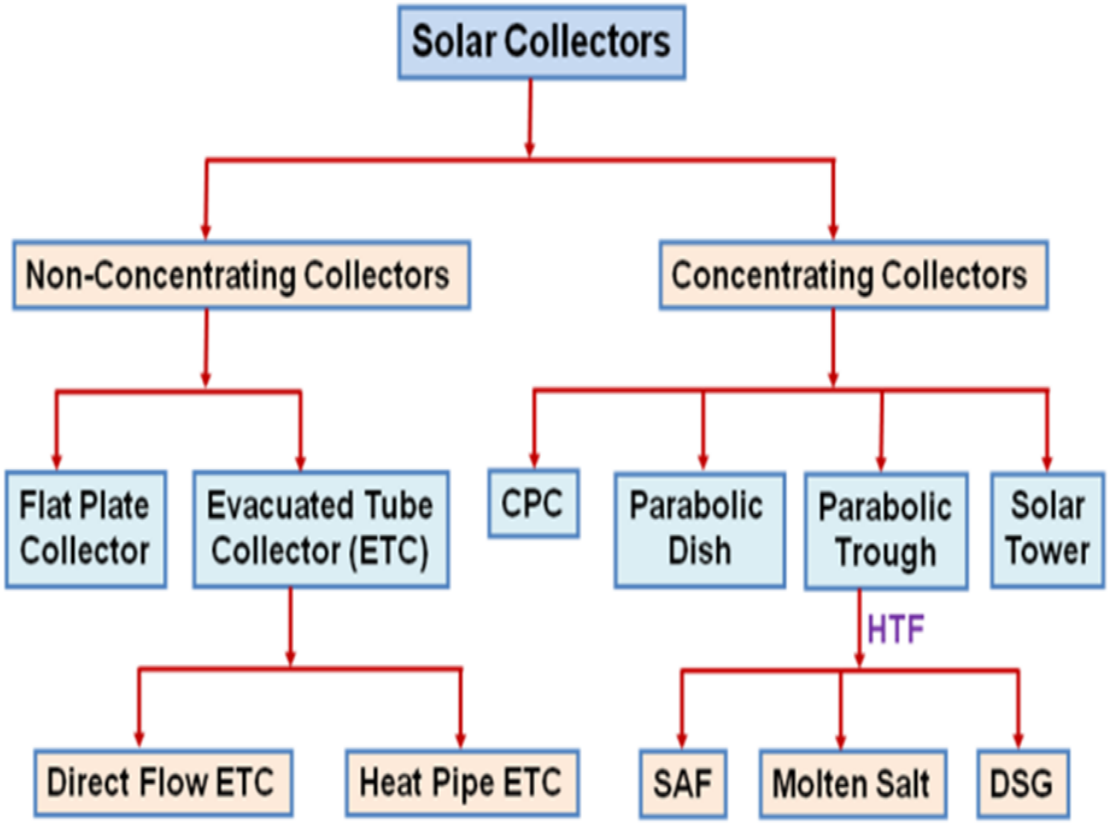

Figure 2.1: Solar Collector Types [12].

2.2 FLAT PLATE COLLECTOR

The heating of water is an example of a fundamental form of solar collector that is used to transport solar energy. It is a development of the fundamental concept of orienting the glass collector in the direction of the solar. The vast majority of the flat panel assemblies consist of two horizontal pipes at the bottom and the top, as well as multiple little pipes that connect them to one another. Always low iron and tempered glass are utilized in the construction of flat panel assemblies. Low iron glass is also sometimes employed. Because glass can remain intact despite exposure to extremely low temperatures, flat panel collectors are among the most long-lasting types of collectors [13]. Flat panel complexes are made up of a black absorber plate, in the lower part of which the pipes and ducts that make up the complex are put.

They are installed in a closed frame that has a see-through cover that is designed to allow some solar radiation to pass through at the top while insulating against heat loss from the bottom. As indicated in Figure 2.2, the black surface is responsible for the absorption of solar energy, while the liquid is supplied by pipes or channels.

Figure 2.2: Flat Plate Collectors [14].

Additionally, the flat-plate collectors can be divided into three distinct sets according to the primary functions that they provide, as detailed below [14]:

a. Used with a too-small increase in temp, like in swimming pools where the solar collector requires no shelter or insulation at the sides or rear. A high flow rate is maintained to restrict the increase in temperature (to ≤ 2°C).

b. Domestic heating and other uses where the ultimate temp needed is not greater than 60°C. The insulation at the rear and at least one transparent shield are essential.

c. Uses for heating process or small-scale power provision, in which temperatures significantly higher than 60°C is essential. Highly sophisticated design methods are required for reducing the losses of heat from the collector to the environment [15].

2.3 EVACUATED TUBE COLLECTORS

Solar collectors that contain thermal pipes, also known as vacuum tubes, are easily accessible on the market. Their operation is distinct from that of other types of solar collectors. Figure 2.3 illustrates how these types of solar collectors work by showing how heat pipes are housed inside of vacuum tubes, which are then sealed off completely and connected at the top to a heat exchanger [16].

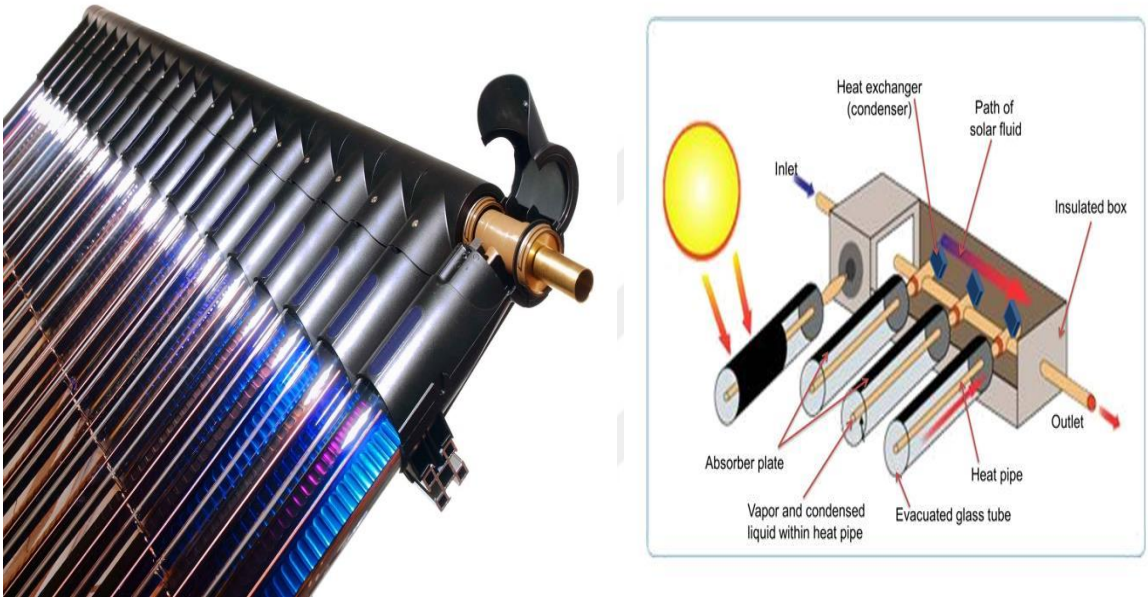

Figure 2.3: Evacuated Tube Collectors [16].

A heat-absorbing collector is several rows of parallel, clear glass tubes that are attached to a header conduit in the evacuated tube collector. The form of these glass cylinders is cylindrical. As a result, the sunshine is always orthogonal to the heat-absorbing tubes, allowing these collectors to function effectively even when there is little sunlight, such as in the early morning or late afternoon, or when there is cloud cover. In regions with chilly, overcast winter weather, evacuated tube collectors are especially helpful.

Copper is used in the construction of these heat pipes, which are then joined by copper fins that have been given a black finish. A metal tip that performs the function of a condenser can be found at the very top of every thermal tube. These solar collectors can work at high temperatures because there is very minimal heat loss. This is made possible by the vacuum

that is present in the space between the thermal pipes, in addition to the impact of transmission on the flow of heat. In addition, the materials that are used in the operation of these solar collectors can change the phase from a liquid to a gaseous state. This gives these solar collectors an edge over other solar collectors because their efficiency is higher than that of other solar collectors [17]. As a result of the high cost, numerous designs have been released onto the market to lower manufacturing costs and increase product longevity. This is accomplished by cutting down on the number of vacuum tubes and making use of reflectors made specifically to concentrate the solar rays on the pipes [18].

2.4 PARABOLIC TROUGH COLLECTORS

The growth of industries based on the production and marketing of these systems, in addition to their installation with various systems, has led to the parabolic trough collectors becoming the most advanced and matured among solar energy technologies in recent years. This has allowed them to be installed with a variety of other systems [18]. As illustrated in Figure 2.4, the manufacturing process for these solar collectors involves bending a sheet of reflective material into the shape of a parabola before covering it with glass tubes to decrease the amount of heat that escapes. When these ponds are oriented toward the solar, the surface of the water is heated by the solar rays, and the solar energy is turned into thermal energy that can be put to productive use.

Figure 2.4: Parabolic Trough Collectors [19].

These technologies have been implemented in multiple settings, including a power plant in Southern California known as the solar power system and a project in southern Spain known as Platform solar de Almeria. Both of these applications are located in the south of the European Union. New advances in the parabolic trough collectors are targeted at reducing the expenses of the companies that manufacture many of these technologies, which are capable of heating the fluid flowing between 50 ℃ and 300 ℃ [19].

Abbas et al, in 2021 presented a mathematical model to calculate the effect of heat transfer and axial temperature distribution of a parabolic trough collector. Found that the results differ numerically based on the tube's twist ratio (4.787) and the presence or lack of twisted tape when using water as the working fluid and the sun energy recorded in Istanbul, Turkey (plain). The position of the study was N longitude 28.97° E and latitude 41°, for 4 recommended months from September to December and from 9:00 am to 3:00 pm. The aluminum absorber tube was reflected with twisted tape at six different angles by the parabolic solar collector's substantial heat gain. Because of the increased surface area and swirling turbulent motion, the Nusselt number, heat transfer, and friction factor were all improved. In comparison to the plain tube, it was discovered that the outlet temperature

increased for twisted tape with 25°, 33°, 45°, 50°, 55°, and 60° by 7.83%, 14.89%, 19.57%, 21%, 4.76%, and 12.23%, respectively. The ideal one is at 50 degrees on the twisted tape. The model uses thermal oil, water, and nanofluids as heat-carrier fluids to calculate thermal efficiency. Findings showed that Nanofluids with independent volume fractions of 0.04 and 0.02 had a greater thermal efficiency than conventional fluids, and their respective effective thermal efficiencies were 80% and 79%. The least effective material is thermal oil, at 76% [20].

2.5 FRESNEL SOLAR COLLECTORS

Fresnel solar collectors are of two types: Fresnel lenticular collectors and Fresnel linear reflectors. The first type is made of plastic material while the second type consists of linear strips of glass that focus the solar light on the receiving line. They can also be installed on flat ground, making the cost of these complexes low compared to other solar collectors as shown in Figure 2.5.

Figure 2.5: Fresnel Solar Collectors [21].

2.6 COMPOSITE EQUIVALENT SOLAR COMPLEX COLLECTORS

Solar collectors that use a composite parabola reflect a significant amount of solar light and channel it toward the elements that are responsible for absorption. Radiation is allowed to

enter the elements of absorption at the bottom of the solar collector by utilizing several inner surfaces that are reflected. The absorbent component can be made in a wide variety of shapes, including those with flat surfaces, double-sided surfaces, cylindrical profiles, or wedge-shaped profiles. Both symmetric and asymmetric designs are available for these solar collectors to choose from. As can be seen in Figure 2.6, composite parabolic solar collectors feature a gap between the element that absorbs solar radiation and the element that reflects it. This gap serves the purpose of preventing the reflection element from drawing heat away from the element that absorbs solar radiation. These solar collectors can be constructed in the form of a single unit with a single hole and one absorption element, or they can be mounted in the form of a panel, and look like solar collectors with a flat panel. Either way, they gather light from the solar [22].

Figure 2.6: Composite Equivalent Solar Complex Collectors [22].

2.7 HELIOSTAT FIELD COLLECTORS

This system's ability to gather solar energy and deliver it to the receiving surface is one of several reasons why it is advantageous to use. This lessens the requirement for the transport of heat energy. In this particular setup, the condensation ratio might range anywhere from

300 to 1500. This suggests that the system operates at a very high level of efficiency. Additionally, the electric power generated by this system is substantial, amounting to more than 10 megawatts (MW). Solar stabilizers are located on the system's surface, and they are responsible for capturing light from the solar and transferring it to the fluid that is moving through the system. Figure 2.7 presents the heliostat solar systems, the primary components of this system involve the piping system, pumps radiation and solar panels.

Figure 2.7: Heliostat Field Collectors [23].

Thermal energy can be stored by heat storage systems, which then provide this energy to electricity-producing systems. Additionally, they keep the process of collecting solar energy distinct from the device that converts it into electricity. These solar collectors are available in three distinct configurations. The solar stabilizers in the first version are completely encircled by the receiving tower in this configuration. The heat is transferred to the fluid that is moving through the receiving surfaces, which have a cylindrical shape and have exterior surfaces that conduct heat. The second method involves the placement of solar stabilizers to the north of the receiving tower in conjunction with receiving surfaces that are able to transfer heat to liquids. The solar stabilizers are positioned to the north of the reception tower

in the third form, and the receiving surface is horizontal and vertical when viewed from the north. [23].

Solar collectors are divided according to the surrounding temperatures and weather conditions, where the solar radiation intensification rate is the same for all solar panels. The first group of panels is represented by the temperature from 30 degrees Celsius to 80 degrees Celsius. As for the second group, the temperature range from 50 degrees Celsius to 200 degrees Celsius. There are groups of panels that operate at temperatures from 60 Celsius to 300 Celsius. In general, the condensation ratio for solar energy beams is 40:10. As for Heliostat solar cell collectors, temperatures range from 300 to 1500. In other types, the condensation ratio is pumping: 10, and the temp is from 60 Celsius to 400 Celsius [24].

2.8 PHOTOVOLTAIC THERMAL (PVT) SYSTEM COMPONENT

The photovoltaic thermal (PVT) system has several moving parts. The solar system consists of an interconnected group of parts that complement each other and are as follows:

2.8.1 Solar Cell

In the manufacturing of solar cells, the use of P-type and N-type silicon, both of which are types of semiconductors, may be seen. Because of the way that it is built, P-type silicon always ends up with one less electron whenever it acquires a new atom. The production of N-type silicon is impossible without the process of atomic mixing, which brings about the addition of a second electron. This leads to the establishment of a depletion zone near the interface [15].

The n-type layer has too many electrons, while the p-type layer has too many holes that are positively charged. N-type and p-type solar cells may be distinguished by the number of electrons present. P-type cells employ boron, which has one less electron than silicon (making the cell positively charged). In an n-type solar cell, phosphorus, which has one extra electron than silicon, is a key component (making it negatively charged). The n-type and p-type layers of a solar cell are shown schematically in Figure 2.8, along with a close-up of the depletion zone that surrounds the junction between the n-type and p-type layers.

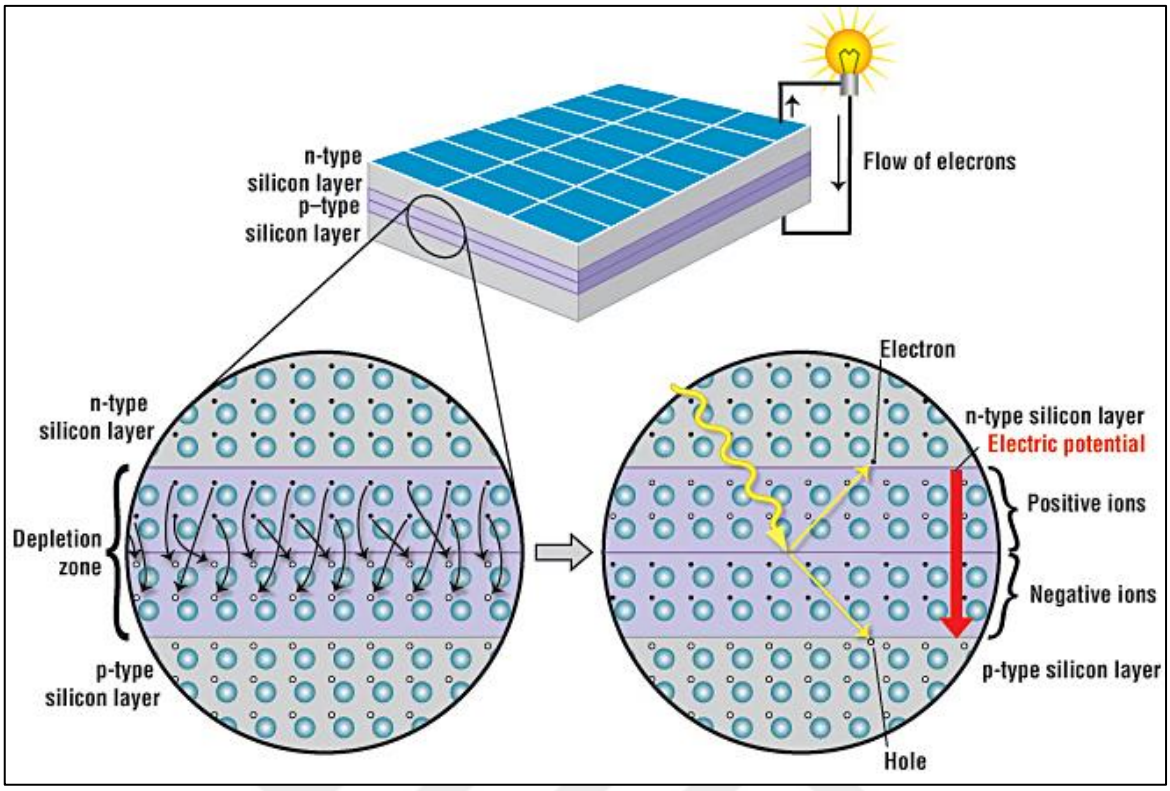

Figure 2.8: N and P Type Layers [15].

A solar cell is a device that captures solar light and converts it directly into electrical energy. A solar cell is around the size of an adult's palm. The color is blue-black and the shape is an octagon. Solar cells are frequently developed in conjunction with solar batteries. Solar modules are the large ones. A solar panel is a casing in which multiple solar cells are built together [25].

The p-type side of the depletion zone, where holes were originally present, is now filled with negatively charged ions, while the n-type side of the depletion zone, where electrons were previously present, is now filled with positively charged ions. These ions' opposing charges provide an internal electric field that inhibits the n-type layer's electrons from filling the p-type layer's holes.

As sunlight hits a solar cell, silicon's electrons are evacuated, which causes "holes" to form the voids the outgoing electrons left behind. The electric field will transport holes to the p-type layer and electrons to the n-type layer if this occurs. Electrons will go from the n-type layer to the p-type layer by crossing the depletion zone and then proceed through the external

wire back of the n-type layer, causing an electrical flow, if the n-type and p-type layers are connected by a metallic wire.

2.9 CLASSIFICATION OF SOLAR SYSTEMS

The solar cells, the controller, and the batteries make up the vast majority of the device's components. Adjusting the inverter so that it can handle alternating currents is something that has to be done if Alternating Current (AC) load delivery is required. In addition to solar panels for homes, solar-powered lighting, cathodic protection, and other photovoltaic (PV) components, an independent PV power plant may also contain the necessary electrical infrastructure to supply electricity to a population located in a remote area. Independent photovoltaic systems may be broken down into a variety of subcategories according to the characteristics of the load. These subcategories include direct current DC systems, AC systems, and AC-DC hybrid systems, among others. The capacity of the system to generate power is the determining factor in each of these classes. The principal fault line that constitutes the majority of the assembly is whether or not there is an inverter [26].

2.10 OPERATING PARAMETERS EFFECT ON PV MODULE PERFORMANCE

PV solar cell transforms light straight into energy. Solar cells have immense potential as a renewable energy source, but their present production costs render them uncompetitive [27]. Consequently, increasing the efficiency [28]. To find a solution, several researchers have employed computational, experimental, and analytic techniques to examine the effect of various operational factors on the degradation of PV module performance. 15% to 20% of photons that reach a PV module are transformed into usable energy, while the other photons just raise the temperature of the cell [29].

When the temp around them increases, the effectiveness of solar panels decreases. In 2006, 2007, and 2008, Sanusi et al. [30-31]. This conclusion is not surprising when one considers the characteristics of the amorphous silicon that is utilized in the production of crystalline silicon cells (a-Si cells). Ray [32] investigated how well photovoltaic (PV) cells worked when subjected to temperatures below freezing. Solar modules comprised of a polymer, copper indium diselenide, and amorphous silicon were subjected to a solar simulator that had a power output of 973 W/m^2 AM 1.5. There is a 25% improvement in performance when

the temperature is 15 degrees Celsius and the tilt is 35 degrees. According to the findings of Malik et al. [33] the spectral response of an (a-Si PV) module and its power output is strongly connected. This plant's strength increases in proportion to the depth of the blue in its surroundings.

The temp of the cells in a monocrystalline solar module is more important than the irradiation spectrum in determining the module's performance. When operating in an indoor environment, the output power of the module decreases by 0.48% when exposed to 500 W/m^2 of solar irradiation, but the same module's output power decreases by 0.5% when operating in an outdoor environment (as observed by Park et al. [32]). Following the observation that the cellular temperature of the module was significantly higher than expected, the conclusion was arrived at. If the surface temperature of a solar panel increases by 1 kelvin, then the panel loses 0.65 percent of its output power, the percent of its fill factor, and 0.08 percent of its electrical efficiency, according to Radziemska [32].

Several factors have a significant impact on the efficiency of photovoltaic (PV) conversion, some of the most important of which are the semiconductor that is utilized, the range of the Solar's spectrum, the spectral sensitivity of the cell, and the reflectivity of the cell surface. Olchowik et al. [36] temperature increases affect the output efficiency of the temperature was raised from 300 K to 330 K, and a drop in efficiency of 15% was seen for monocrystalline PV cells; however, Kumar and Rosen [37] reported only a decrease in efficiency of 5% for a-Si PV cells. Ugwuoke and Okeke [38] discovered that under conditions of 600 W/m^2 of irradiation dropped by approximately 31 percent. When the temperature of the module grew from 25 to 50 degrees Celsius, Jong et al. [39] discovered the PV responses based on numerical analysis. Keeping a close check on the module as it was being heated allowed that to be discovered. The pace at which dark current travels through the module accelerates in tandem with the rise in temperature of the module. This results in a rise in both the short-circuit current and the free-carrier losses. The output performance of the photovoltaic (PV) module that was employed in the investigation that was conducted by Malik et al. in 2010 was thus below average.

The forward voltage of the PV cell decreased by 2 mV for every degree that the operating temperature increased, but the forward voltage of the silicon diode only decreased by 1 mV

for every degree that the operating temperature increased. The forward current of the PV cell, on the other hand, was maintained at a constant level of 100 mA during the whole procedure. When being used in an environment with temperatures ranging from 295 to 375 degrees Kelvin (K). Researchers working under the direction of Shenck [40] it was discovered that when temperatures increased, photovoltaic (PV) systems saw a decrease in both their efficiency and the output power that they produced. This was a direct consequence of the fact that the band gap of the atoms shrunk as the temperature increased. This was an unavoidable end result as a direct result of the fact that the temperature rose [41].

In an analytical study, Singh and Rabindra [41] and Tonui and Trip Anagnostopoulos [42] studied the impact of natural and forced airflows on the PV panel's efficiency which was 12.5% when the cell was at 26 degrees Celsius and only 9% when the cell temperature was 68 degrees Celsius. They determined that a 15 cm finned air channel with a flow rate of 60 m^3/hr could achieve a thermal efficiency of 30%. A thin metal sheet has a thermal effect at 28%, while a typical cooling system was 25%. Qunzhi and Leilei [42] conducted an experiment that demonstrated using a water cooling system. The researchers are the system for cooling solar panels by adding new elements on the surfaces of thermal conductivity, which increased the efficiency of heat transmission very significantly. This method has been accustomed to the basic concepts of the transmission of thermos, but with the nature of the two obstacles and problems, the most important of which is the difficulty of the possibility of manufacturing surfaces and complaining about it that makes them easy to use in solar energy.

Teo et al. [46] discovered that when a polycrystalline PV system was not cooled, its efficiency was only 8%-9%, in this paper, the researchers improved the performance of the photovoltaic cell using various means. The researchers used materials added to water to improve heat transfer. It is normal for the additives to absorb more heat generated from the generation of electrical energy in the solar panel, many obstacles and obstacles prevented the use of these additives, the most important of which is the high specific weight of the materials that slow the movement of water. This was done by directing a steady airstream via a duct connected to the PV device's back layer.

When the researchers Bahaidarah et al. [47] adopted an efficient strategy for water-cooling the module, in this research, the researchers combined the properties of heat-emitting surfaces with the properties of the water used. The process of combining characteristics gives positive hybrid and improved results. The percentage of improvement reached 20%. During this period, the module's cell efficiency grew by up to 9%. To do this, the module's rear panel was outfitted with a heat exchanger mechanism. The mathematical predictions and the experimental facts are strikingly consistent with one another. Thanks to the use of a cotton-wick cooling structure in conjunction with a variety of coolants, Chandrasekar et al. [48] were able to reduce the cell temperature of a PV module by 30%. The module's power output rose by 6.5 watts while its electrical efficiency increased by 1.4%. Using this method, solar modules were able to reach greater levels of thermal and electrical efficiency.

Valeh-e-Sheyda and colleagues [49] combined the flow of water and air through a microchannel in their cooling system to reduce the temperature of the PV module's cells. This resulted in a 38% increase in the amount of electricity that the module could emit. Water was fed through a heat exchanger panel using the module's electrical efficiency increased significantly, rising from 10% to 13% as a result of the adjustment. When the solar module was not cooled, just 10% of its potential electrical production could be collected. Ceylan and his colleagues [50] have written up and published the findings of their investigation. Alami [51, 31] was able to lower the temperature of a photovoltaic (PV) device by applying an artificial layer of mud to the bottom of a PV cell. This layer consisting of water molecules was placed at the bottom of the PV device. The heat was then equally dispersed across the surface of the cell by evaporation. As a direct result, the output power and voltage of the solar cell were 8.2%, 9.01%, and 9.75%, respectively, when it was cooled with water, as opposed to being uncooled. Compared to the condition in which the module was not cooled at all, this was an improvement.

2.11 HEAT TRANSFER SPECIFICATION

The basic idea of heat transfer depends on the temperature difference between the two surfaces. The speed of heat transfer and the amount of heat transferred depends on several factors, the most important of which are the type of medium, its thickness, and the speed of

movement, as in the use of water or air. Most of the materials used are water and air because of their high heat transfer properties, in addition to their cheapness and availability [52].

3. METHODOLOGY

3.1 INTRODUCTION

The means of generating clean energy are considered one of the latest trends today, as the scientific and technical authorities are interested in cooperating with researchers and experts in finding the best ways to generate clean energy to preserve the environment and preserve human resources at the same time. From this principle, many tools have been developed to generate clean energy, the most important of which are solar panels. Solar panels have taken a large part in scientific research due to their high efficiency and cheap price, in addition to the ease of installing their equipment. However, with the development of use, many obstacles appeared in these systems, the most important of which is the high temperature of the board. Many researchers have developed means of cooling solar panels, starting with air, and currently paying attention to using water.

The system proposed in the study (PVT-collector design) is compared to that of conventional systems (thermal collector, and PV panel). Recent additions to this subject use a matrix to characterize the transient temperature distribution of a PVT system water cooler. This location's flow is responsible for turbulent flow. The working formulas of mass, momentum and energy conservation were simultaneously applied to the water. Consequently, this chapter applies computational fluid dynamics to examine heat transfer from solar PV to cooling water. Several techniques and computerized algorithms are utilized to solve and assess water flow issues. The objective of this study is to develop a numerical model capable of predicting heat transfer characteristics to examine heat changes under a variety of conditions. The parts that follow describe the experimental setup, the PVT-collector design, and the testing and evaluation methods.

3.2 EXPERIMENTAL SETUP

Solar energy has been one of the most accessible and economical renewable energy sources during the last decade. Solar thermal collectors and photovoltaics are mature solar energy collection technologies. Photovoltaics, on the other hand, lose efficiency at higher operating temperatures, and solar thermal collectors have limited exergy. As a result, Photovoltaic Thermal (PVT) collectors were created, which combine the advantages of photovoltaic cells

and solar thermal collectors into a single device. The PVT collector is built experimentally and placed next to the other thermal collector. The first is a standard PV panel in its own area, which may be used to evaluate and compare the thermal and electrical efficiency of other systems. June and July are the warmest months of the year, with highs of 48°C.

The prototype, as shown in Figures 3.1 and 3.2, was created with a separate solar thermal collector connected to a storage tank. Cold water is provided from a source to the PVT systems via flexible plastic piping, and hot water is fed from the PVT system to the tank via flexible plastic piping. Water is circulated throughout the system using a water pump. Separate PV panels and PV panels combined in PVT collectors are connected to a voltmeter, an ammeter, and a separate thermometer to measure voltage and current, as well as the temperatures of the water and PV panels.

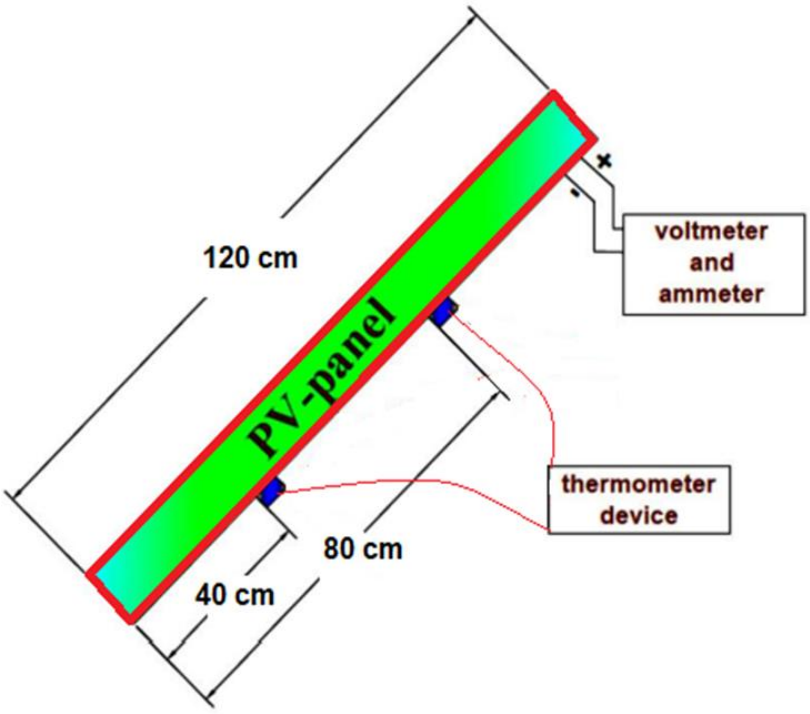

Figure 3.1: Schematic of PV Testing.

As shown in Figure 3.1, the used PV-panel dimensions are 120 cm for the length of the panel and the thermometers subjected in the back of the panel at 40 cm and 80 cm height. At the back of the panel, the current wires are connected and it allows the user to connect a

voltmeter device. This system can be used to measure the generated current and measure the generated heat on the surface of the panel.

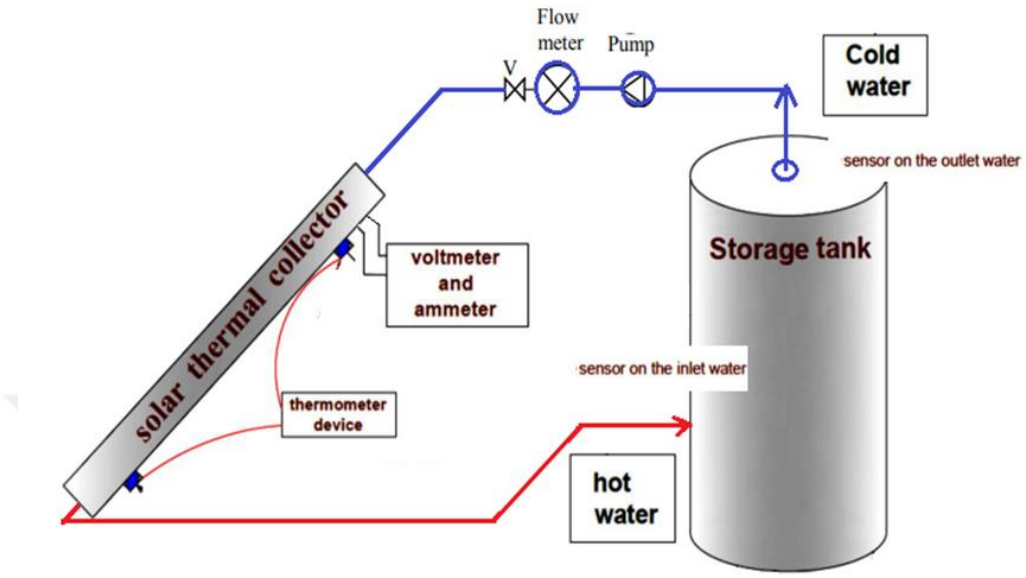

Figure 3.2: Schematic of the Closed Loop System for PVT Testing.

As shown in Figures 3.1 and 3.2 the used system in this work. It contains a water tank, water pump, solar panel, thermostat (two types of thermostats), valves and copper pipes. There are numerous ways to remove heat. The earliest and most prevalent refrigeration method is based on water. It is also possible to do the task using air, a combination of water and air, or other fluids. There have been studies [18] including the use of internal gases or even vacuum to reduce heat loss. To transport all of the thermal radiation to the liquid, air, or gas with the highest efficiency, it is important to avoid heat losses. Additionally, heat transfer circuits can be classified as either open-flow through or closed-loop. In addition to these categories, there are two types of collector geometry: flat plate collectors and tube collectors. Finally, it can find solar collectors with integrated storage, meaning the tank is positioned in the same region as the collector or a system in which the tank is not integrated and is located elsewhere. All of this suggests that each collector technology correlates to specific temperature levels and applications that are appropriate. These components are the principal heat transmission modes (between all solid layers). Figure 3.3 illustrates each component of a PVT glazed door.

Figure 3.3: Experimental Prototype of all System: PVT Collector.

3.3 PVT COLLECTOR PANEL

The photovoltaic panel type employed for the experiment is depicted in Figure 3.4.

Figure 3.4: PV Panel Used in Experiments.

Table 3.1 shows the panel's properties as measured under standard test conditions.

Table 3.1: Data Specification of the PV Panel.

Maximum Power	100 Watt
Power Tolerance Ranger	+/- 3%
Open Circuit Voltage	21.5 V+/- 3%
Short Circuit Current	6.46 A+/- 4%
Maximum series fues	12 A
Maximum power Volt	17.5 V
Maximum power current	5.7 A
Weight	7 kg
Operating temperature	-40 ºC to + 85 ºC
Dimensions	1200x540x30
Application class	A+

3.4 THE PRESENT SYSTEM COMPONENT

Experiments include two types of copper tube design, the first type is shown in Figure 3.5 and the second type is shown in Figure 3.6. The main reason for using two types of tube shapes is to know the effect of the tube shape on the cooling efficiency of the solar panel, as

changing the shape is related to the length of the tube path and the nature of the heat transfer from the panel to the water. As for the selection of copper pipes, it is known that copper is a good conductor of electricity, so it was adopted in the experiments devoted to this work. The independent copper pipes in the experiments of this thesis are shown in Figures 3.5 and 3.6.

Figure 3.5: U-Shape Copper Pipe Model.

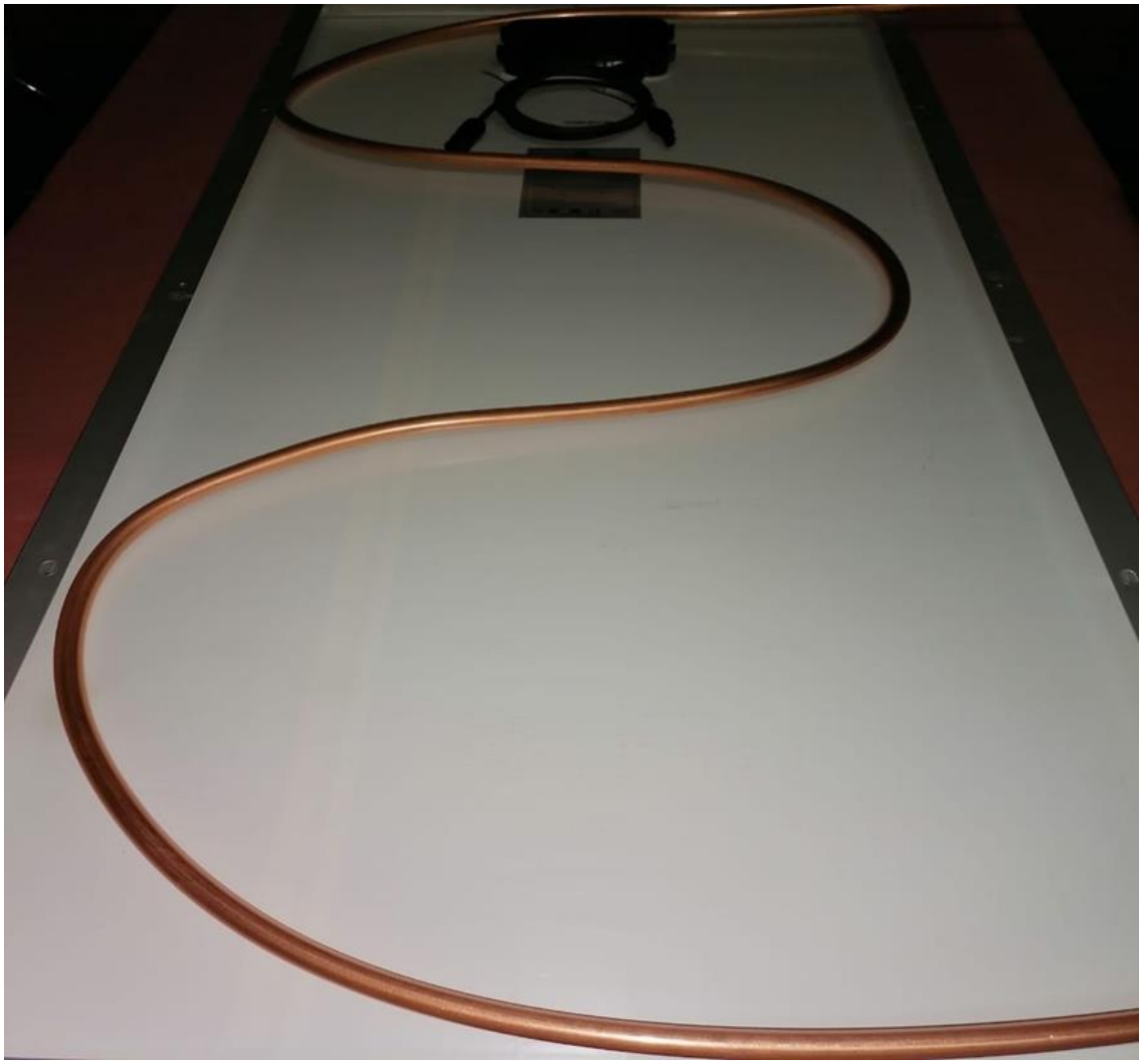

Figure 3.6: S-Shape Copper Pipe Model.

Heat is transferred from the PV panel to the water cooling system through a copper tube. Copper tubing is frequently used in heating and cooling systems. Copper tubing is classified into two types: soft and rigid. Copper tubing is linked using flare connections, compression connections, pushed connections, and solder. Copper is highly corrosion-resistant, yet it is becoming increasingly expensive. Soft copper is used in this investigation, as seen in Figures 3.7 and 3.8.

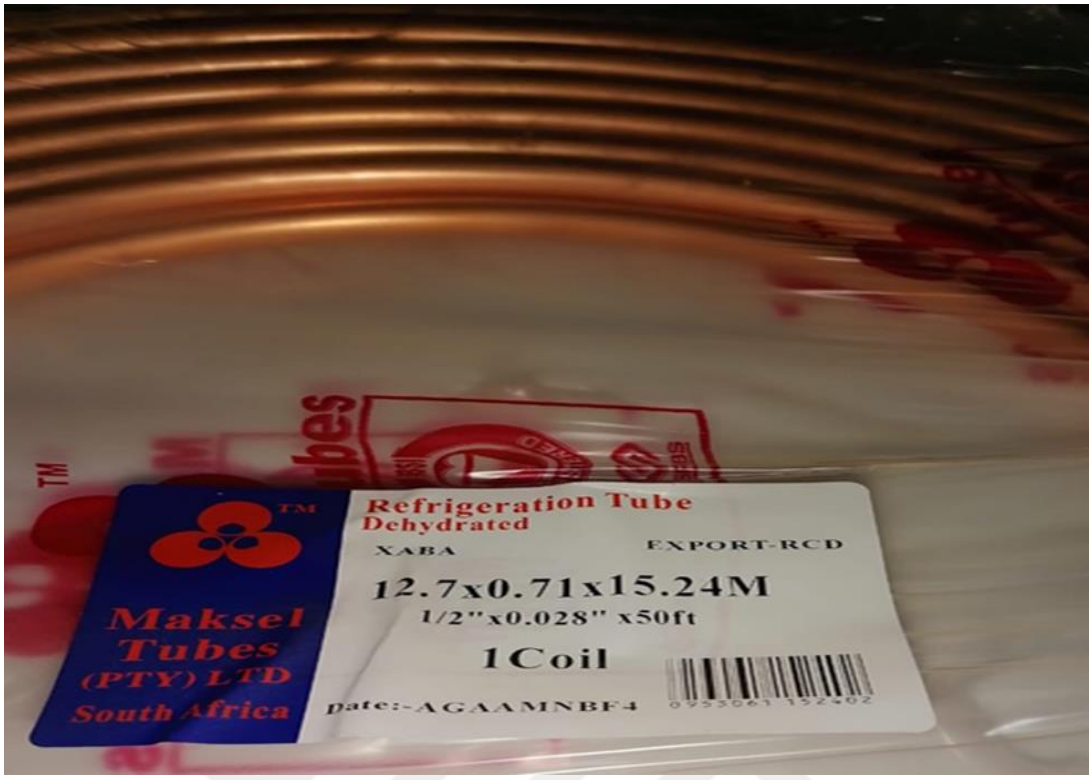

Figure 3.7: The Copper Tube Used In This Research.

Figure 3.8: The Copper Tube Size.

The soft copper tubing with the size of ½ inch (12.7 mm) diameter and 0.8 mm thickness is used to produce the coils. This type of tube can be bent easily to travel around the PV panel in the path of the tubing as shown in Figure 3.9.

Figure 3.9: Bending Process of the Copper Tube.

3.5 THE STORAGE TANK

To achieve optimal heat exchange between the water and the surface of the solar panel and to ensure the cooling process and heat transfer in a regular manner, a water tank was connected to the cooling system. The main work of the water tank is to control the transfer of temperatures and to control the process of measuring the temperature of the water entering and leaving the panel dynamically. To ensure the water circulation process, a small water pump is attached to circulate the water, in addition to a lock position to control the flow. Figure 3.10 illustrates the experiment's utilized storage tanks. It is produced for household usage in an Iraqi facility and has a capacity of 60 L.

Figure 3.10: The Storage Tank.

The reservoir is an essential part of the system, as laboratory experiments cannot be conducted without the presence of the reservoir. Therefore, the specifications of the tank must be appropriate to the size of the system. In addition, the tank is insulated with glass wool to transfer heat from the tank to the surroundings. The purpose of this is to maintain the accuracy of the heat transferred to the water from the solar panels to the tank. Table 3.2 outlines the tank's specifications.

Table 3.2: The Tank Dimensions.

The outer diameter of the tank (cm)	43
The inner diameter of the tank (cm)	35
The volume of the tank (l)	60
Outer thickness (mm)	0.4
The thickness of insulation material (cm)	4
Inner tank thickness (mm)	2
The diameter of pipes (in)	¾

3.6 MEASUREMENTS

3.6.1 Measuring the System Voltage and Current

The current and voltage produced by the two separate PV panels are measured using two voltmeters and two ammeters at different times and with varied solar radiation values. Current and voltage are recorded when a variable resistive load is connected to plot the current-voltage and power-voltage curves for each PV panel.

3.6.2 Measuring the System Temperature Differences

Several temperatures have been detected using a thermocouple sensor connected to a thermometer instrument. They are the temperatures of the thermal collector and the PVT collector's inlet and outlet water, and the temperature of the Paraffin wax inside the PVT collector in two positions. Measuring the temperature of the PV panel combined with the PVT collector in two positions, and the temperature of the separate PV panel in two positions, as well as the ambient temperature.

The main objective of this study is to measure temperature changes on the surface of the solar panel, and to achieve this goal, two thermometers were placed on the solar panel. Dimensions were set by dividing the solar panel into three equal parts, and sensors were installed on the panel.

Figure 3.11 shows the position of the thermostat that is used to measure the PV-panel temperature. The importance of these thermostats is to measure the surface temperature which represents the surface temperature of the copper pipes.

Figure 3.11: Thermal Sensor Position at the PV Panel.

In addition to the above-mentioned thermometers, a manual thermometer was used to measure the temperature from a distance. In the first case, the devices can be seen installed on the back of the solar panel, while the portable device is used to measure the surface facing the sun. Also, the inside and outside water temperatures were measured by a special thermometer as shown in Figure 3.12.

Figure 3.12: Panel Surface Temperature Measurement.

The next step is to measure the water flow circulation at different points to find the heat absorbed by the water system. For that, many thermostats are fixed at different points in the cooling water system. As shown in Figure 3.13, the first water thermostat was fixed in the tank inlet water.

Figure 3.13: Cold Water Tank Pipe with Thermometer.

Figure 3.14 measure the outlet water temperature. It is clear from the differences in the amount of heat absorbed by the water.

Figure 3.14: Hot Water Tank Pipe with Thermometer.

3.6.3 Solar Radiation Measurement

The countless interactions that take place between the many components that make up the atmosphere each contribute to a gradual depletion of the atmosphere's overall strength. On average, only approximately a third of the total quantity of radiation that originates in space really makes its way to Earth. This percentage decreases as move farther away from Earth. Radiative transfer is a term that describes not only the modeling of the optical processes that affect solar radiation inside the atmosphere but also the description of the optical processes that have an influence on solar radiation within the atmosphere. A computer is being used to perform both the description and the modeling.

The process of absorption takes place in the atmosphere and involves the transformation of the energy into another form after it has been absorbed by a particular component at a certain wavelength. This transformation takes place as part of the absorption process. The

atmosphere is the location where the process of absorption takes place. Because of this transformation, the light no longer possesses the same amount of energy that it did before. Absorption can take place at very precise wavelengths, which are referred to as absorption lines, or it can take place throughout a large spectrum of wavelengths. Both of these scenarios are possible.

The concept of "absorption lines" can be applied to any of these two circumstances. When light interacts with a variety of different substances at the same wavelength, a physical phenomenon known as scattering may take place. Scattering can take place at any wavelength. This encounter may take place in a variety of distinct ways depending on the circumstances.

Particles and molecules are responsible for the energy of an incident wave being refracted and reradiated in all directions, which, in the end, leads to the wave's energy being depleted. The scattering pattern provides an illustration of the probability that a photon moves along a certain route.

This pattern is controlled not only by the size and shape of the particles or molecules that are scattering but also by the wavelength of the light that is being projected upon them. Specifically, the larger the particles or molecules that are scattering, the more light be scattered. The angle that the solar makes with the zenith affects the optical route that the radiation takes and plays an important part in the process of radiative transfer. This takes place irrespective of whether or not there are clouds in the sky. The optical path is shortened and the amount of radiation that is obliterated is decreased when the zenithal angle of the solar is reduced.

The clearness index is determined by dividing the amount of radiation received at ground level by the amount of radiation received at the top of the atmosphere. It is a quantity without dimensions that can be specified for any wavelength, spectral interval, or time interval [20]. Typical values range from 0.1 to 0.7 to 0.8 for extremely cloudy conditions and clear skies, respectively. In clear skies, aerosols and water vapor are the primary contributors to ozone depletion. Due to scattering and absorption by aerosols and molecules in such environments, approximately 20% to 30% of total extraterrestrial radiation is lost throughout its welling path. This quantity fluctuates with wavelength, and when solar radiation moves through the atmosphere, its spectral distribution shifts.

Clouds are the major depleting elements in the atmosphere, hence they play a significant role. The optical qualities of clouds vary: optically thin clouds allow a considerable amount of energy to reach the earth, whereas optically thick clouds create darkness by blocking downward radiation. To a first approximation, clouds are spectrally neutral, meaning that their presence does not alter the spectral distribution of radiation. Direct radiation is the radiation that comes from the direction of the solar [20]. At the top of the atmosphere, there is just direct radiation. At ground level, a portion of this direct radiation is absorbed by a horizontal surface. It also gets radiation diffused by atmospheric elements and coming from the sky vault in all directions, except solar radiation, which has already been accounted for. Multi-source radiation is referred to as diffuse radiation. Global radiation is the combination of direct and diffuse radiation. Figure 3.15 displays the solar radiation detection instrument.

Figure 3.15: Solar Radiation Detection Instrument.

The system uses a series of equations to find the efficiency, which is one of the important steps in this research. The current research is based on several basic factors, the most important of which are the temperature of the plate, the ambient temperature, and the intensity of the solar's brightness on the plate. These factors are included in a series of equations that combine with the temperature of the water used to cool the solar panel. The

equations below show the type of mathematical relationships that be used to find the results [28]:

$$E_{th} = M_w \times C_p \times \Delta T \tag{3.1}$$

$$\Delta T = T_3 - T_4 \tag{3.2}$$

$$M_w = V_w \times \rho \times (T) \tag{3.3}$$

$$\eta_{th} = \frac{100 \times E_{th}}{A_m \times C_p} \tag{3.4}$$

Where E_{th} is thermal energy, M_w is mass flowrate of water, C_p is specific of gravity of water, ΔT is water differences, T_3 is inlet water temperature, T_4 is outlet water temperature, V_w is water velocity, ρ is water density, η_{th} is thermal efficiency, and Am is pipe area

3.6.4 Extraterrestrial Solar Radiation

The quantity of energy that the Sun's electromagnetic radiation distributes to a certain location over time is referred to as solar radiation intensity. In addition to visible light, this energy also comprises ultraviolet and infrared radiation.

A number of variables, including the time of day, the season, the latitude, the altitude, the amount of cloud cover, and the atmospheric conditions, affect how much solar radiation reaches the Earth's surface. For instance, solar radiation is stronger at noon than it is in the morning or evening, and it is stronger at the equator than it is at the poles. Human activities, such as the release of greenhouse gases that trap some of the incoming radiation in the atmosphere, can also have an impact on the intensity of solar radiation [53].

Watts per square meter (W/m^2) is the unit used to express the intensity of solar radiation. The solar constant, also known as the average solar radiation intensity at the top of the Earth's atmosphere, is approximately 1361 W/m^2. However, based on the aforementioned variables, different amounts of solar radiation actually reach the Earth's surface.

Extraterrestrial radiation is the term used to describe the solar radiation that enters the Earth's atmosphere. The Sun's activity and the changing distance between the Earth and Sun both affect the intensity of extraterrestrial solar radiation. Throughout the course of a year, this radiation's value fluctuates between 1307 (W/m^2) and 1393 (W/m^2).

The following formula may be used to determine the intensity of alien solar radiation that strikes the Earth's surface and is directed at a right angle to the direction of solar energy [54]:

$$I_{on} = I_{sc} \frac{r}{R^2} \tag{3.5}$$

Where r is the Earth's intermediate distance from the Sun, R is the Earth's immediate distance from the Sun, I_{SC} is the solar constant I_{SC} = (1353±21) [55]

The following formula may be used to determine the amount of alien solar radiation energy that falls directly on a square meter of surface in a unit of time:

$$I_{on} = \left[1 + 0.0333 \cos \frac{360n}{365}\right] I_{sc} \tag{3.6}$$

Where n is a day in a year that counts from January 1st.

The energy of extraterrestrial radiation on horizontal surfaces can be calculated as follows:

$$I_{oh} = I_{on} + \cos z \tag{3.7}$$

Where z is the zenith angle (the angle between direct solar beams and a line that is right-angled on a horizontal surface). Zenith angle (z) can be calculated as follows:

$$\cos z = \sin \alpha = \sin L \sin \delta + \cos L \cos \delta \cos h \tag{3.8}$$

By substitution of equation (3.6) in equation (3.7) the energy of extraterrestrial radiation o on a horizontal surface for a particular day in a year can be calculated as follows:

$$I_{oH} = I_{sc} \left[1 + 0.0333 \cos \frac{360n}{365}\right] (\sin L \sin \delta + \cos L \cos \delta \cos h) \tag{3.9}$$

Where I_{sc} is the solar constant, n is a day in a year that counts from January 1st, L is the local latitude, δ is the declination, and h is the hour angle.

Hour measure (one hour, minute, or second) is the most common way to represent the hour angle (h), also stated in degrees and radians. The apparent motion of the Sun along the circles parallel to the equator and the change in observation location both affect the hour angle. Calculating the hour angle magnitude (h) is as follows:

$$h = \pm\frac{1}{4}(\text{number of minutes from local solar time}) \tag{3.10}$$

The + sign applies to afternoon hours and the − sign to morning hours. The maximum value of the declination angle is δ = 23° 27′. It comes with June 21st (summer's longest daylight in the northern hemisphere, i.e., winter's shortest daylight in the southern hemisphere). The minimal value of declination angle δ = − 23° 27′ comes up with December 20th (summer's longest daylight in the southern hemisphere, i.e., winter's shortest daylight in the northern hemisphere). During the spring and autumn equinox, on March 21st and September 22nd the declination angle is 0°. The declination value (δ) can be calculated for every day in a year as follows:

$$\delta = 23.45 \sin\left[\frac{360}{365}(284 + n)\right] \tag{3.11}$$

Where n is a day in the year (1 ≤ n ≤ 365).

The whole daily extraterrestrial radiation from the sunrise to the sunset can be calculated as follows:

$$I_0 = \frac{24}{\pi} I_{sc}\left[1 + 0.0333\cos\frac{360n}{365}\right]\left[\cos L\cos\delta\cos h_s + \left[\frac{2\pi h_s}{360}\right]\sin L\sin\delta\right] \tag{3.12}$$

Where h_s is the time of sunrise (sunset) beyond the horizon.

In order to define the daily amount of energy of solar radiation on surfaces on the Earth, it is necessary to define the time of sunrise and sunset (h_S) beyond the horizon. In the moment of sunrise (sunset) beyond the horizon the height angle of sun α has 0 magnitudes. By the substitution α = 0 in the following equation [56]:

$$\sin\alpha = 0 = \sin L\sin\delta = \cos L\cos\delta\cos h_s \tag{3.13}$$

$$\cos h_s = -tgL \times tg\delta \tag{3.14}$$

The equation (3.14) can be solved for h_S if $-1 \leq -tg\delta\ tgL \leq 1$.

$$h_s = arc\cos(-tgL\ tg\delta) \tag{3.15}$$

The equation (3.15) has two solutions:

$$h_{s\ sunrise} = -h_s\ and\ h_{s\ sunset} = h_s \tag{3.16}$$

Where hS *sunrise* and hS *sunset* are hour angles of sunrise and sunset. If: $-tg\delta\ tgL > 1$, the Sun will not rise whole day (the Polar Night); $-tg\delta\ tgL < -1$, the Sun will shine the whole day (the polar day). Using the already obtained expressions for sunrise and sunset hour angles, the length of a day (time from sunrise to sunset beyond the horizon) can be calculated as follows [57]:

$$t_{day} = \frac{2}{15}\cos^{-1}(-tgL\ tg\delta) \tag{3.17}$$

4. RESULTS AND DISCUSSION

4.1 INTRODUCTION

The temperature of the water discharged from the PVT system was monitored, and the findings showed that the reaction was satisfactory. The current method calculated the thermal efficiency of the PVT water collector and compared the results to those of previous research to validate the simulation findings of the PVT system design. It discussed a valid test model in the previous chapter; this chapter describes the results of tests run using that model. The investigation of the behavior of solar heat transmission to fluid flow over a wide temperature range and with various flow effects to identify how it operates as a heat transfer mechanism. Continue with this and apply it to a broader range of working scenarios to gain a deeper understanding of heat transfer behavior and the reasons for heat transfer deterioration, which is one of the most important goals of this project. The current findings can be divided into three categories. The first group presents the validation of this study. The second category is known as the water velocity effect, consisting of different water velocity levels related to the temperature being employed. The third group's presentation discusses the impact of solar irradiation's heat on the PVT water system.

4.2 SOLAR RADIATION INTENSITY

The intensity of solar radiation determines the amount of energy the sun delivers in a given amount of time. The information is used to create and assemble solar energy systems in a variety of sectors. The researcher measures the amount of solar light falling on specific areas at various times of the year. The amount of solar light falling on places with similar climates at the same latitude is then calculated [58]. The most common methods for measuring solar energy are total radiation on a horizontal surface or total radiation on a solar-tracking surface. The daily solar radiation intensity in Iraq, Baghdad, is depicted in Table 4.1 and Figure 4.1.

Table 4.1: Daily Solar Radiation Intensity in Iraq, Baghdad.

Time (h)	February Intensity (W/m^2)	March Intensity (W/m^2)	April Intensity (W/m^2)
5	0.00	0.00	0.00
6	0.00	0.00	20.59
7	146.39	85.94	176.35
8	320.57	262.28	260.49
9	470.66	438.63	463.69
10	500.07	577.38	582.75
11	574.11	673.16	731.35
12	591.36	732.24	766.26
13	539.63	726.87	737.61
14	444.28	668.69	672.27
15	325.20	516.51	542.47
16	150.09	357.17	406.40
17	146.39	161.13	238.11
18	0.00	0.00	86.83
19	0.00	0.00	0.00

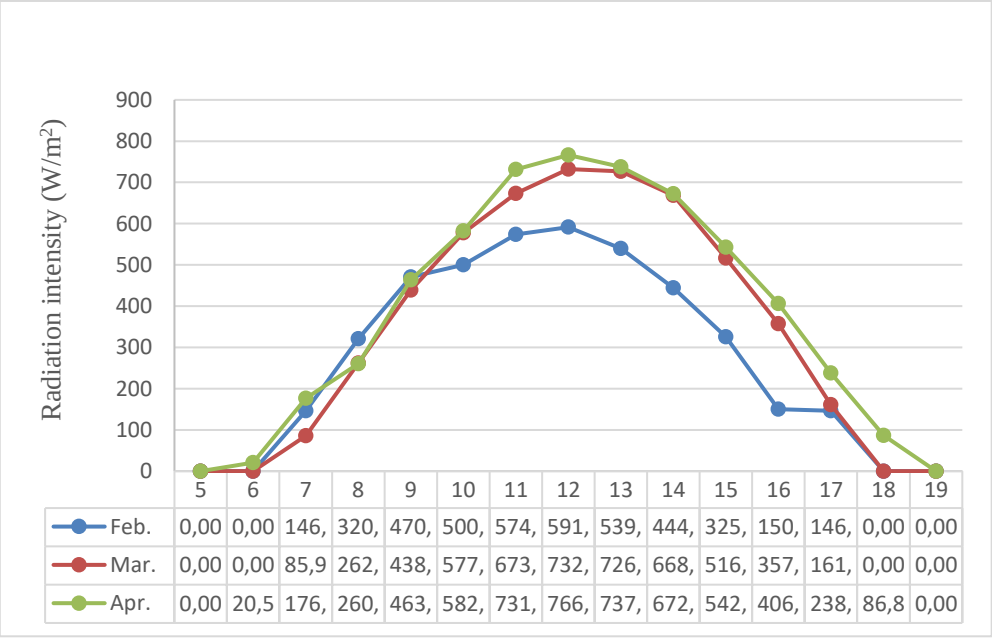

Figure 4.1: Solar Radiation Intensity in Iraq, Baghdad.

The total solar radiation intensity in Iraq, Baghdad in three months are sown in Figure 4.2.

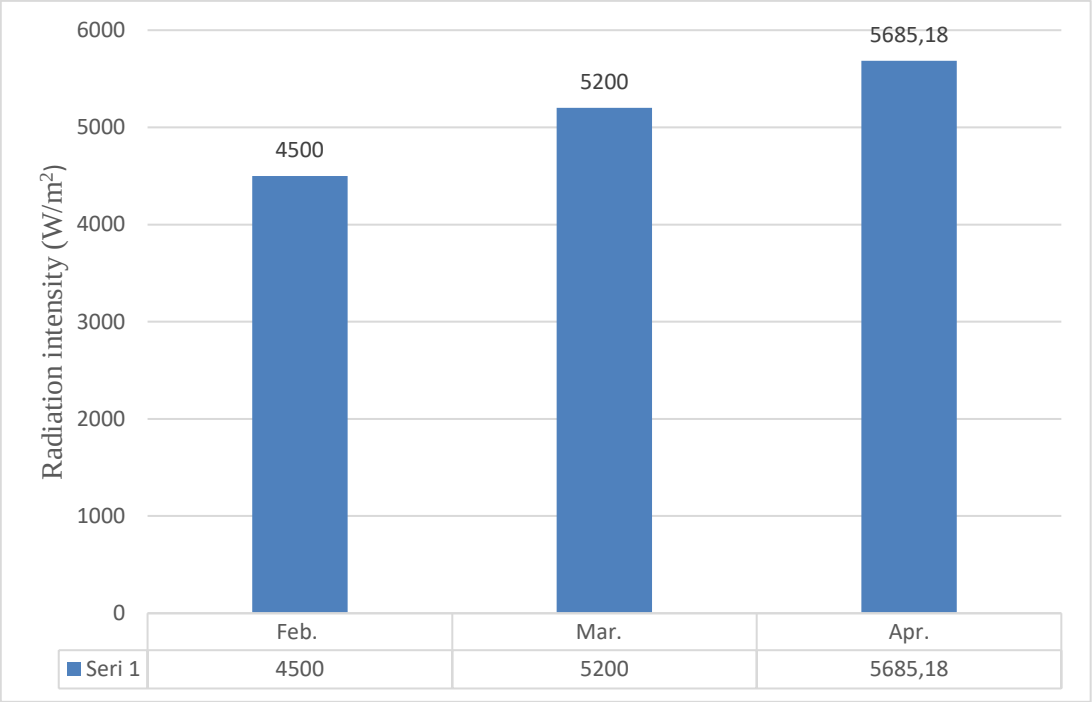

Figure 4.2: Total Solar Radiation Intensity in Iraq, Baghdad.

These measurements have been used in this thesis as an input data

4.3 COMPARISON WITH PREVIOUS STUDIES

In this research, all tests were conducted in Baghdad, Iraq. Only three months were chosen to conduct the research. Therefore, the researcher recorded the temperatures and compared them with what has been established in global locations for the average temperature of the city of Baghdad. The aim of temperature recording is that it plays an important role in the temperature of the cooling water used in the cooling system. The table below shows average temperatures.

Table 4.2: Variations in the Temperature in Iraq, Baghdad [58].

Month	February	March	April
Average Maximum Temperature (°C)	21.0	25.0	31.0
Average Temperature (°C)	15.0	19.0	24.5
Average Minimum Temperature (°C)	9.0	13.0	18.0

The system employs a set of equations to determine efficiency, which is one of the most significant responsibilities in this line of research. The current study is based on several essential factors, the most important of which are the temperature of the plate, the temperature of the surrounding environment, and the intensity of the solar's brilliance on the plate.

To achieve the intended effect, these components are accounted for in a set of equations and combined with the temperature of the water flowing through the solar panel. The equations presented in chapter three show the types of mathematical relationships that be used to arrive at the results. And by comparing the results reached by the researcher with the results presented by Mohd Rosli and others in 2018, it is possible to note the convergence between the results in the case of the serpentine absorber of both studies. The same conditions have been used such as the solar irradiation 1000W/m^2 and the water flow rate was 0.0001 to 0.005 kg/s.

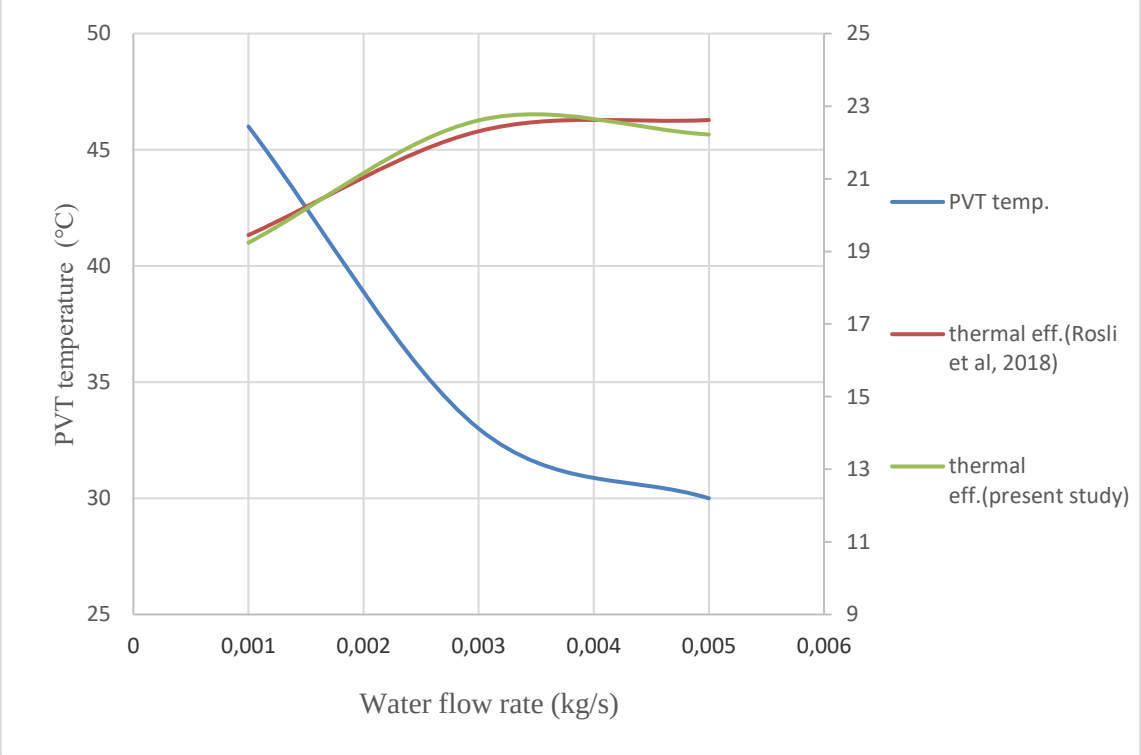

Figure 4.3: Plot of Comparison of Temperature Differences and Thermal Efficiency for Serpentine Absorber with The Different Mass Flow.

It can be seen that the water temperature rises in the copper cooling tubes and the direct relationship between flow velocity and temperature. It can also be seen that the surface temperature of the solar panel decreases with the increase in water flow. Based on the results, the researcher continues with the system tests.

4.4 MASS FLOW RATE EFFECT

As a PVT water system, the PVT water collector is designed and built with a flow channel absorber design. At varied mass flow rates and based on the compared data of mass flow rate and temp differences from the previous studies as shown in the previous section the researcher selected the water flow rate values for experiments. In this research, the daily solar radiation intensity in Iraq, Baghdad were measured by the researcher using solar radiation detection instrument and compared with Hamad et al, (2022) presented in [53], and the dimensions and shapes selected from Rosli et al, (2018). The measured data applied in the formulas presented in chapter three (equation 3.1 to equation 3.5), finally the water flow (0.02 kg/s) was selected from Misha et al, presented in [28] and the mass flow 0.01 kg/s taken from the researcher to measure the differences because its more suitable to the cooling pipe diameter.. The radiation levels vary based on the boundary circumstances during design and selection as shown in Figure 4.4. All the other data such as the PV panel dimensions and pipe dimensions taken from the real measurement of the system component. The examination of the dynamic properties of the thermal effect in the absorption domain is known as PVT model analysis. It aids in the selection of a PV cooling system. It is shown in Table 4.3 below.

Table 4.3: The Cases of the Present Study.

	Temperature (°C)	**Water flow (kg\s)**	**Case Figure**
First case	18 to 26	0.01, 0.02	
Second case	18 to 26	0.01, 0.02	

The experiments are carried out as described in chapter three, and the results demonstrate that solar radiation, ambient temp, and mass flow rate had an impact on the performance of the PVT cell temp. These effects ranged from 0.01 to 0.02 depending on the average cell temp of the PV panel, the PVT water collector, and the ambient temp. The thermal absorber and water flow both work to lower the temp of the PVT water-collecting cell. According to Figure 4.4, the thermal absorber and water flow lower the temp of the PVT water collecting cell.

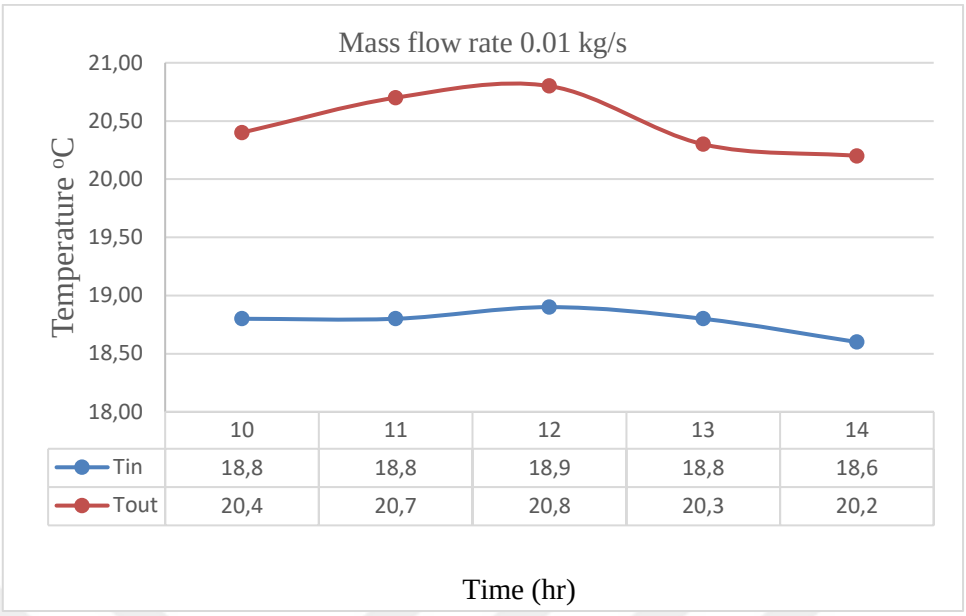

Figure 4.4: Differences in Temperature of Inlet-Outlet Cooling Pipe System Using Water Flow 0.01 Kg/S in February Month.

It can be noticed in the figure the results of the mass flow rate tests in the copper cooling tubes at a speed of 0.01 kg/s. The results observed that the maximum differences in the temp are at 12 o'clock which represents the highest thermal load. The water flow temperature reached 20.8 ℃ and the difference in temp in the cooling system is 1.9 ℃. Accordingly, all the calculations that were mentioned in the laws presented in the third chapter were completed, and then the water flow in the copper tubes was increased to 0.02 kg/s. The results appear in Figure 4.5.

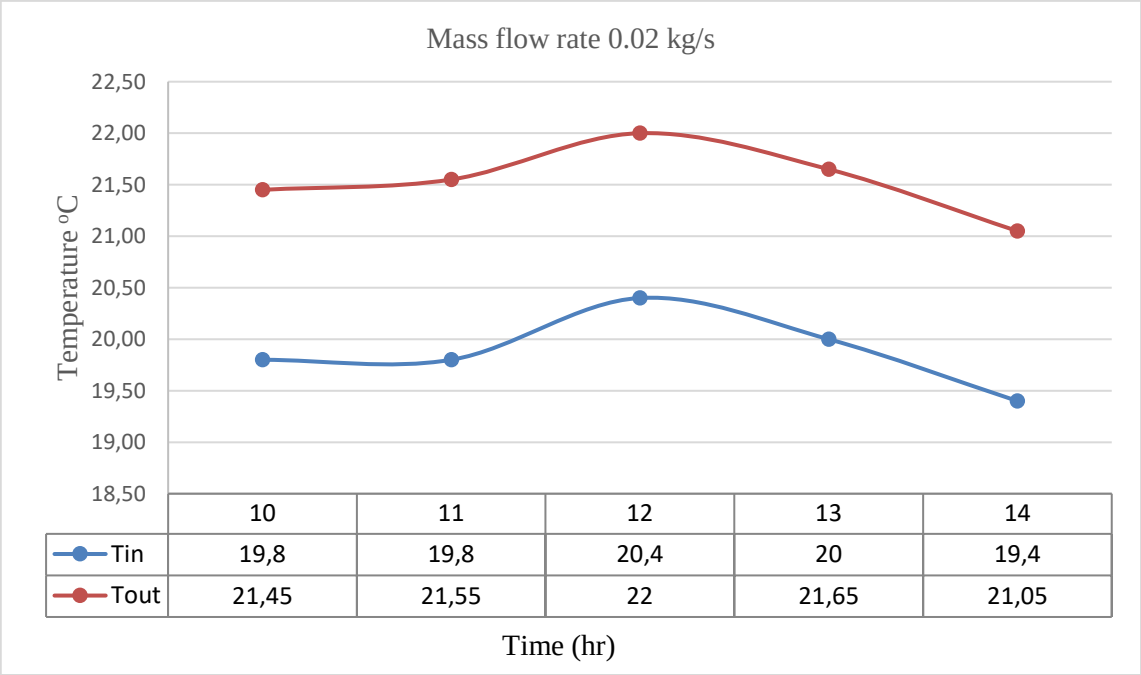

	10	11	12	13	14
Tin	19,8	19,8	20,4	20	19,4
Tout	21,45	21,55	22	21,65	21,05

Figure 4.5: Differences in Temperature of Inlet-Outlet Cooling Pipe System Using Water Flow 0.02 Kg/S in February Month.

In this case, the results observed that the maximum differences in the temp. Are at 12 o'clock also, which is mean that in Iraq country, the thermal load must be calculated at this time. The water flow temp reached 22℃ and the difference in temp in the cooling system is 1.6 ℃. When comparing the results shown in Figure 4.4 and figure 4.5 can observe a differences in temp in rage of 1.66 ℃ between input and output of the cooling pipe system. These differences will be used in calculation of equation 3.2. Also, the range of temp differences between the water mass-flow of 0.01 and 0.02 kg/s was 1.06 ℃ which is show the differences in heat transfer based on flow speed. The next step is to calculate the thermal efficiency were shown in Figure 4.6.

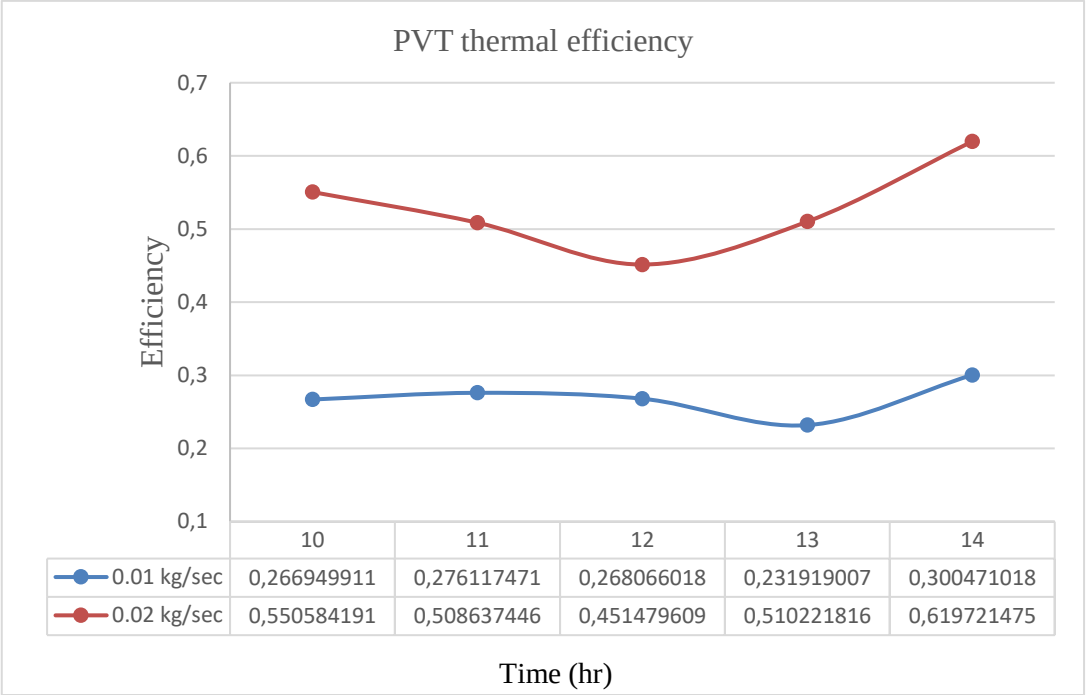

Figure 4.6: PVT Thermal Efficiency Differences in February Month**.**

It is clear from figure 4.6 that the minimum efficiency difference was at 12 o'clock. The efficiency difference reaches 18% while it reaches 32% at 14 o'clock. The weakness in thermal efficiency at 12 o'clock is due to the high differences in the panel temp. The counters demonstrate a direct relationship between the change in mass flow and the drop in cell temp in the PVT water system. The effect of varying water velocities is a crucial factor that influences the overall process of heat transfer. Results demonstrate the findings of studies undertaken to assess how the speed of the water influenced the collecting pipes. This suggests that the water's speed absorbs some of the heat delivered from the PV down the pipe.

The PVT water collector may create both heat and power. As a result, the temp of the output water after heat gain and the device's thermal efficiency are the measurements used as indications of thermal performance within the scope of this study. According to the data, there is a negative relationship between the change in mass flow rate and the temp of the exit water. To generate warm water with higher thermal efficiency, the flow rate must be kept constant between 0.01 and 0.02 kg/s.

The average thermal efficiency is proportional to the temp differential between the water being pumped in and the water being pumped out, and this ratio varies with the mass flow rate values. As the mass flow rate increases, the temp difference between the water's point of entry and point of exit decreases. The temp difference between the water's entry and exit points can be decreased by raising the mass flow rate while also boosting thermal efficiency. The same procedure was repeated in March month and April month. The results are presented in Figures 4.7 to 4.12.

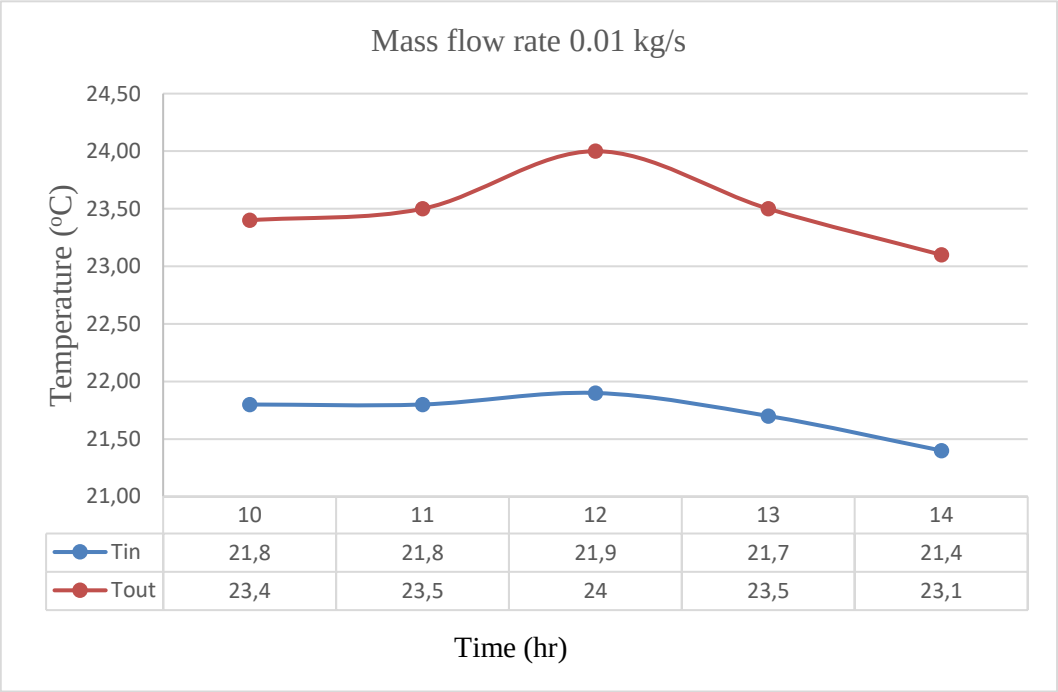

Figure 4.7: Differences in Temperature of Inlet-Outlet Cooling Pipe System Using Water Flow 0.01 Kg/S in March Month.

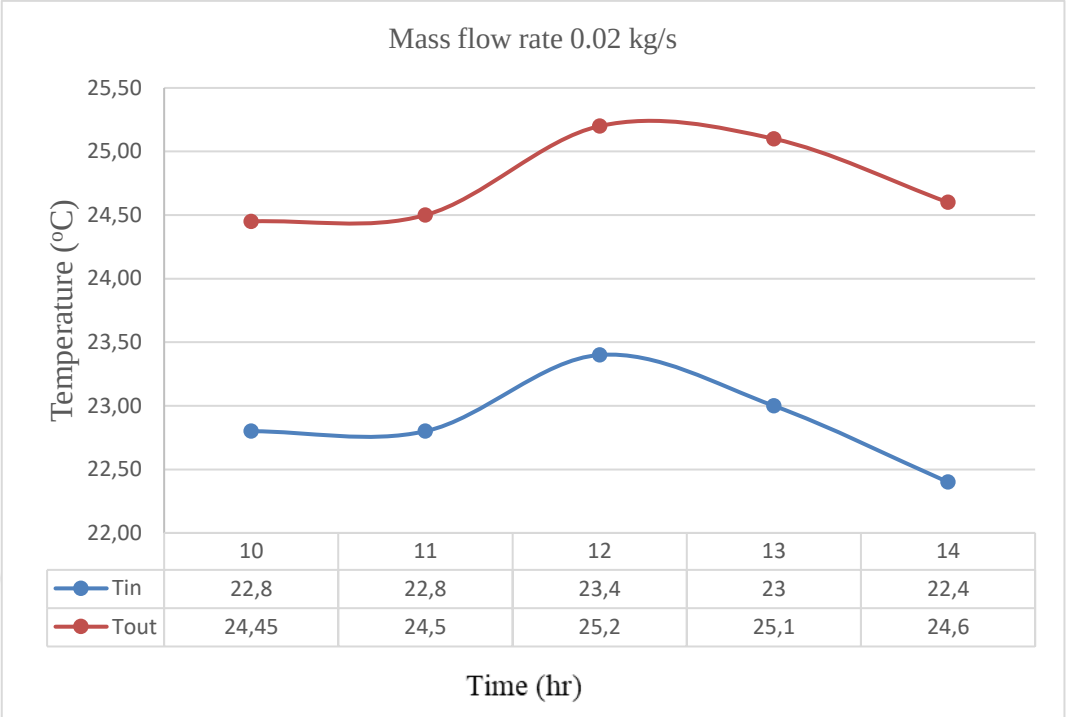

Figure 4.8: Differences in Temperature of Inlet-Outlet Cooling Pipe System Using Water Flow 0.02 Kg/S in March Month.

In March month, the results in Figure 4.7 and Figure 4.8 observe that the maximum differences in the temp are also at 12 o'clock as in February month which represents also the highest thermal load. The water flow temp reached 24 ℃ at 0.01 kg/s water flow rate and 25.2 at 0.02 kg/s water flow rate. The differences in temp in the cooling system are 2.8 ℃.and 1.8 ℃ in both cases.

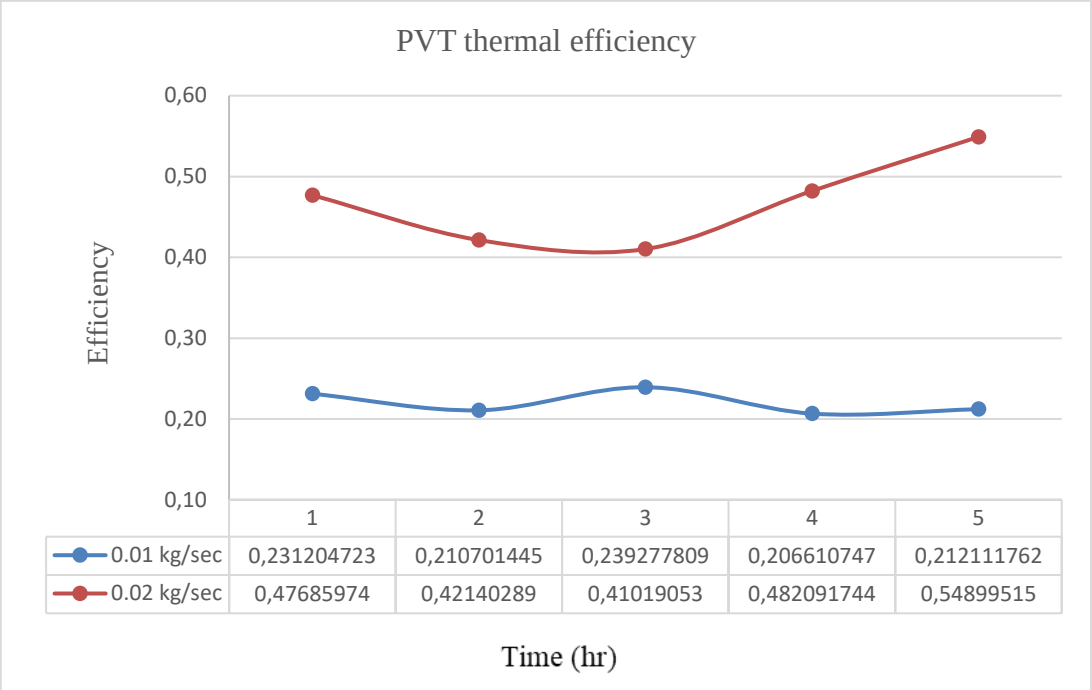

Figure 4.9: PVT Thermal Efficiency Differences in March Month.

Figure 4.9 displays the hourly fluctuations in electrical efficiency from mass flow rate throughout the course of the months. It is clear that the electrical efficiency for both systems varied in direct relation to outside temperature. Yet, compared to 0.01 kg/sec mass flow rate, electrical efficiency for 0.02 kg/sec is much greater. It is clear from figure 4.9 that the minimum efficiency difference also was at 12 o'clock. The efficiency difference reaches 17% while it reaches 34% at 14 o'clock. The weakness in thermal efficiency at 12 o'clock is due to the high differences in the panel temp as presented previously.

Finally, in April month, the results in Figure 4.10 and Figure 4.11 observe that the maximum differences in the temp also at 12 o'clock as in February month which represents also the highest thermal load. The water flow temp reached 28.85 ℃ at 0.01 kg/s water flow rate and 29.1 at 0.02 kg/s water flow rate. The differences in temp in the cooling system are 2.18 ℃.and 1.7 ℃ in both cases.

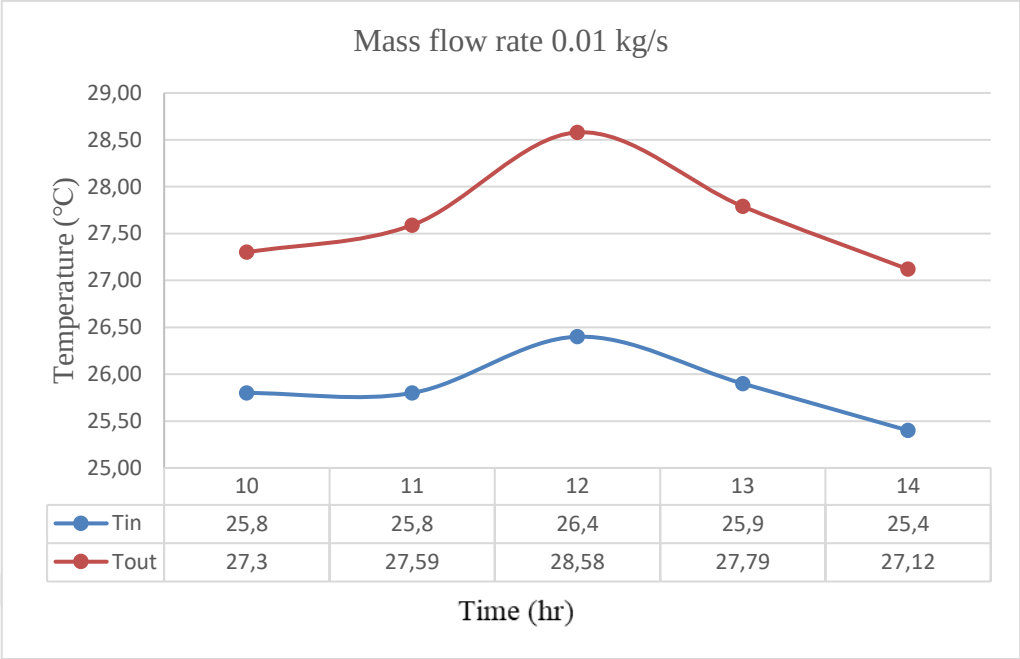

Figure 4.10: Differences in Temperature of Inlet-Outlet Cooling Pipe System Using Water Flow 0.01 Kg/S in April Month.

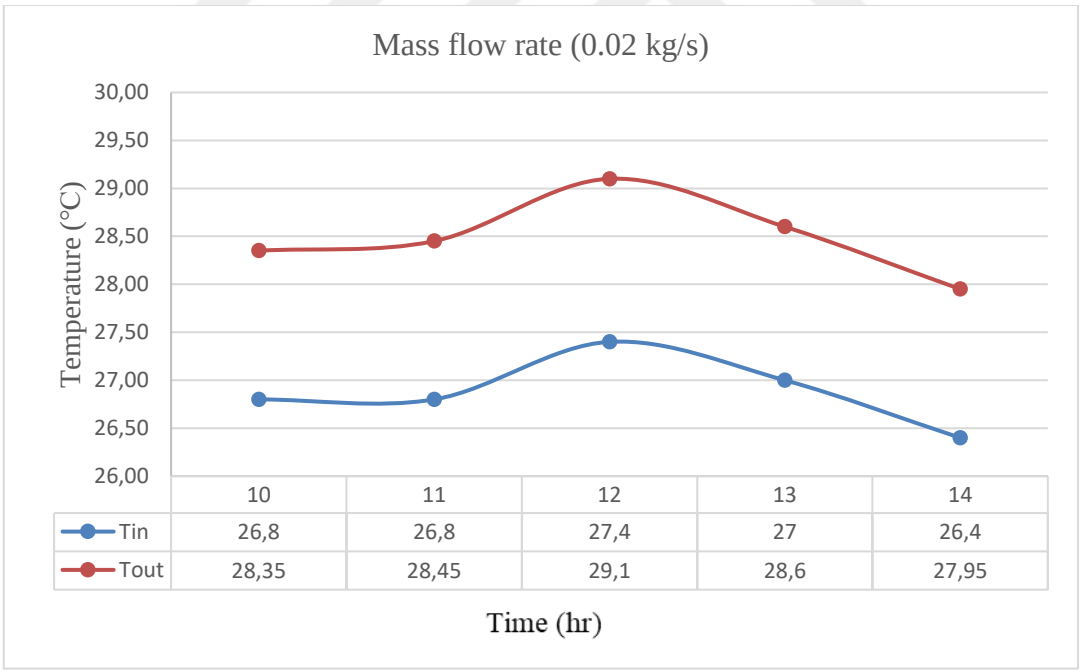

Figure 4.11: Differences in Temperature of Inlet-Outlet Cooling Pipe System Using Water Flow 0.02 kg/s in April Month.

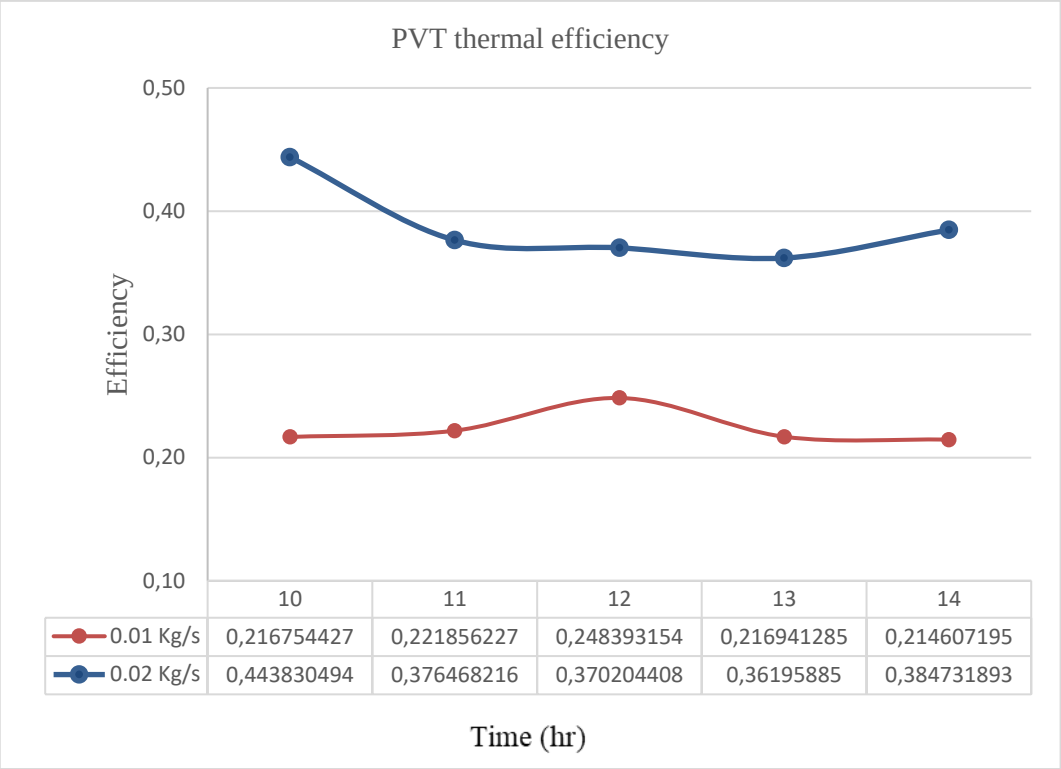

Figure 4.12: PVT Thermal Efficiency Differences in April Month.

The thermal efficiency calculations shown in Figure 4.12 observed that that the minimum efficiency difference also was at 12 o'clock. The efficiency difference reaches 12% while it reaches 17% at 14 o'clock. The weakness in thermal efficiency at 12 o'clock is due to the high differences in the panel temp. The figures show that the increase in water flow rates is directly proportional to the rate of heat absorption. That is, the increase in the flow of water in the copper tubes has increased the heat absorption in the solar panel. This, in turn, had a positive effect on the efficiency of the solar panel. For that Figure 4.13 shows the results in thermal efficiency of all cases of the present study.

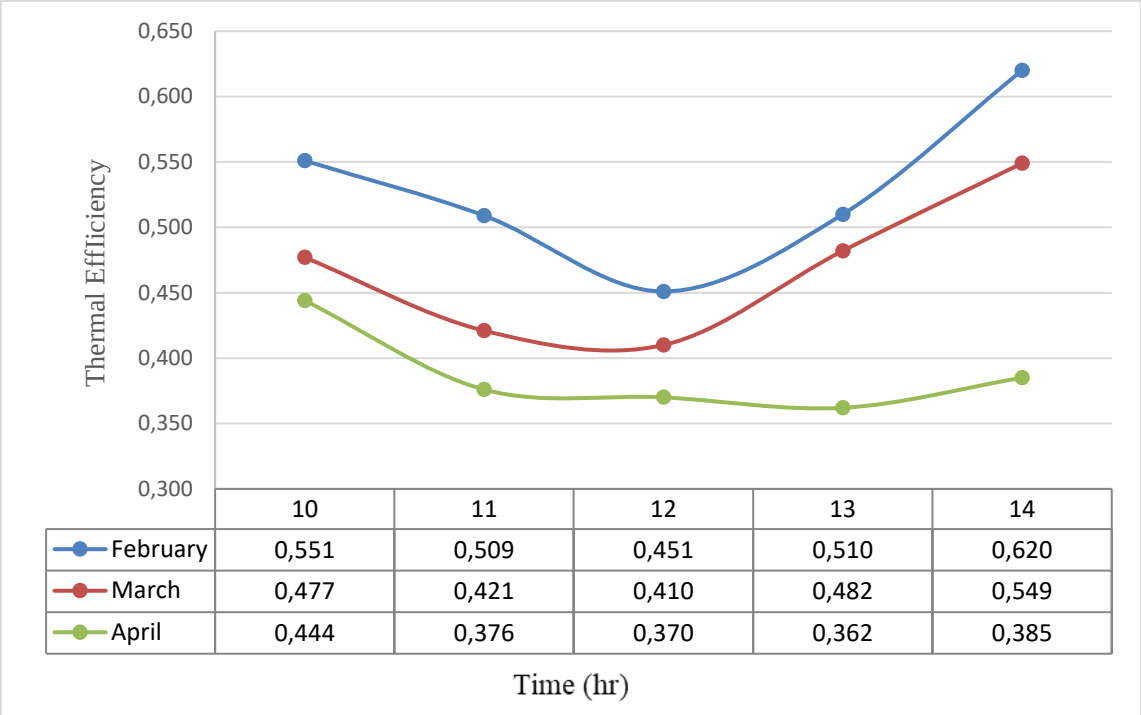

	10	11	12	13	14
February	0,551	0,509	0,451	0,510	0,620
March	0,477	0,421	0,410	0,482	0,549
April	0,444	0,376	0,370	0,362	0,385

Figure 4.13: A Comparison of Thermal Efficiency of Different Months.

Solar cells operate under different weather conditions. The most important of which is the change in the intensity of solar radiation. Therefore, the intensity of solar radiation was compared with the efficiency of the solar panels in all of the below. PVT water collectors can produce both electrical and thermal energy. As a result, the output water temperature and the thermal efficiency of the device are used to assess its effectiveness. The results reveal that when the mass flow rate increases, the temp of the outflowing water falls. The flow of 0.02 kg/s is observed more efficient heat absorption than 0.01 kg/s and the increase in efficiency was about 0.3% of thermal efficiency.

When the mass flow rate changes, the average thermal efficiency demonstrates how well the system handles the temp difference between the entering and exiting waters. The temp difference between entering and departing water may reduce as the volume of water moving through a given area increases. Increases in mass flow rates enhance thermal efficiency, which is measured by how much warmer the incoming water is than the existing water. The PVT water collector, which also generates energy and heat, serves an important use in the home by supplying hot water.

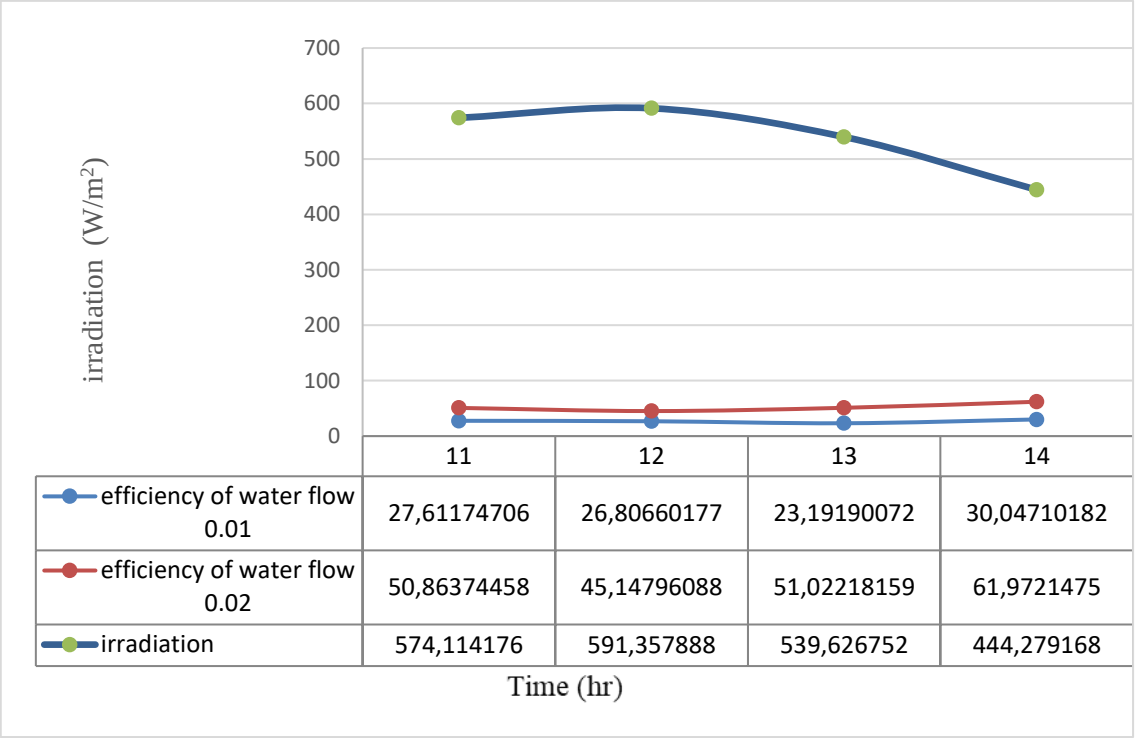

Figure 4.14: A Comparison of Thermal Efficiency of Different Mass Flow Rate and Irradiation.

The Figure shows that irradiation has a direct thermal effect on the thermal efficiency. And in all cases, the higher mass flow rate increases the thermal efficiency. As a result, the output water temp and the thermal efficiency of the device are used to assess its effectiveness. The average water temp at the PVT system's output and input change when the intake water temp changes. The results reveal that when the mass flow rate increases, the temperature of the outflowing water falls. Because average thermal efficiency is determined by the temp difference between the input and output, it varies with the mass flow rate. The thermal efficiency (as measured by the temp differential between the entering and departing streams) improves as the amount of water passing through the system increases.

5. CONCLUSIONS

The performance of a PVT system equipped with a dual absorber was analyzed as part of this research project. The results of the experiments that were carried out in the Iraqi climate are used as the foundation for the numerical analysis that is undertaken. In this study, the performance of the PVT system was evaluated and compared to that of earlier research. The primary takeaway from the recently completed research project is that the PVT system achieves its best level of thermal efficiency when operating at a mass flow rate of 0.02 kg/s. Additionally, as can be seen from the obtained data, the improved serpentine design pipes are a design that is effective due to the higher thermal efficiency they provide. The conclusion of the present work can be summarized below:

In February month, the results of 0.01 kg/s water mass flow rate observe that the maximum differences in the temperature are at 12 o'clock which represents the highest thermal load. The water flow temperature reached 20.8 ℃ and the difference in temperature in the cooling system is 1.9 ℃. When the mass flow rate is 0.02 kg/s, the maximum differences in the temperature are at 12 o'clock also, which is mean that in Iraq country, the thermal load must be calculated at this time. The water flow temperature reached 22℃ and the difference in temperature in the cooling system is 1.6 ℃. The minimum efficiency difference was at 12 o'clock. The efficiency difference reaches 18% while it reaches 32% at 14 o'clock. The weakness in thermal efficiency at 12 o'clock is due to the high differences in the panel temperature.

In March month, the results observed that the maximum differences in the temperature are also at 12 o'clock as in February month which represents also the highest thermal load. The water flow temperature reached 24 ℃ at 0.01 kg/s water flow rate and 25.2 at 0.02 kg/s water flow rate. The differences in temperature in the cooling system are 2.8 ℃. And 1.8 ℃ in both cases. The minimum efficiency difference also was at 12 o'clock. The efficiency difference reaches 17% while it reaches 34% at 14 o'clock. The weakness in thermal efficiency at 12 o'clock is due to the high differences in the panel temperature as presented previously.

In April month, the results observed that the maximum differences in the temperature also at 12 o'clock as in February month which represents also the highest thermal load. The water

flow temperature reached 28.85 ℃ at 0.01 kg/s water flow rate and 29.1 at 0.02 kg/s water flow rate. The difference in temperature in the cooling system is 2.18 ℃. And 1.7 ℃ in both cases.

The thermal efficiency calculations observed that the minimum efficiency difference also was at 12 o'clock. The efficiency difference reaches 12% while it reaches 17% at 14 o'clock. The weakness in thermal efficiency at 12 o'clock is due to the high differences in the panel temperature.

The results reveal that when the mass flow rate increases, the temperature of the outflowing water falls. The flow of 0.02 kg/s observed more efficient heat absorption than 0.01 kg/s and the increase in efficiency was about 0.3% of thermal efficiency, and irradiation has a direct thermal effect on the thermal efficiency.

REFERENCES

[1] A. D'Angola et al., "Theoretical and numerical study of a photovoltaic system with active fluid cooling by a fully-coupled 3D thermal and electric model," Energies, vol. 13, no. 4, 2020, doi: 10.3390/en13040852.

[2] A. Pavlovic, C. Fragasa, M. Bertodi, and V. Mikhych, "Thermal Behavior of Monorystalline Silicon Solar Cell: A Numrical and Exprimental Investigation on the Modle Encapsultion Material," J. Appl. Comput. Mech., vol. 7, no. 3, pp. 147-155, 2021, doi: 10.2055/jacm.221.3782.3101.

[3] G. Omeroglu, "CFD analysis and electrical efficiency improvement of a hybrid PV/T panel cooled by forced air circulation," Int. J. Photenergy, vol. 2018 doi: 10.115/2018/939683.

[4] M. G. Noxpnco, J. Wilton, and S. Rff, "A review of the recent development of photovoltaic/thermal (Pv/t) systems and their applications," Futur. Cities Environ., vol. 6, no. 1, pp. 1-16, 2020, doi: 10.5334/fce.97.

[5] K. Sopian, A. H. A. Alwali, and H. A. Kazm, "Novel Designs of Photovoltaic Thermal (PV/1) Systems," Int. J. Recent Technol. Eng., vol. 8, no. 4, pp. 623-629, 2019, doi: 10.35940/ijrte.d5144.118419.

[6] A. M. Elbrek, K. Sopin, A. Fazlizan, and A. Ibrahim, "An innovative technique of passive cooling PV module using lapping fins and planner reflector," Case Study Thrmal Engnerring, vol. 19, no. January, p. 100607, 2020, doi: 10.1016/j.csite.2020.100607.

[7] M. S. Alobaid, "Determining the performance characteristics of flat plate and photovoltaic thermal collector for sustainable cooling systems integration," p. 183, 2019, [Online]. Available: http://etheses.whiterose.ac.uk/22948/.

[8] G. Raina and N. S. Thakur, "Mathematical Approach for Optimizing Heat Sink for Cooling of Solar PV Module," vol. 7, no. 2, pp. 62–66, 2019.

[9] K. E. Walters, "Thesis Computational Fluid Dynamics (Cfd) Modeling For Cdte Solar Cell Manufacturing Submitted by," p. 81, 2011, [Online]. Available:

https://mountainscholar.org/bitstream/handle/10217/52132/Walters_colostate_0053N_10741.pdf?sequence=1&isAllowed=y.

[10] H. H. Al-Kayiem and S. T. Mohammad, “Potential of renewable energy resources with an emphasis on solar power in Iraq: An outlook,” Resources, vol. 8, no. 1, pp. 1–20, 2019, doi: 10.3390/resources8010042.

[11] Mena, Ali, & İbrahim, KOÇ. Phase Change Material (PCM) Effect on Photovoltaic Performance of Solar Panels. AURUM Journal of Engineering Systems and Architecture, 2021, 5(2), 211-223.

[12] N. Selvakumar, H. C. Barshilia, & K. S. Rajam. “Review of sputter deposited mid-to high-temperature solar selective coatings for flat plate/evacuated tube collectors and solar thermal power generation applications.” NAL Project Document SE, 2010,1025.

[13] M. Irwanto, “Solar irradiance and optimum tilt angle of photovoltaic module in Tanjung Morawa, North Sumatera, Indonesia,” Int. J. Res. Adv. Eng. Technol. Online, vol. 1, no. December, pp. 2455–0876, 2015, [Online]. Available: https://www.researchgate.net/publication/311886785.

[14] L. W. Thong, S. Murugan, P. K. Ng, and C. C. Solar, “Energy efficiency analysis of photovoltaic panel on its operating temperature,” J. Eng. Appl. Sci., vol. 12, no. 14, pp. 3692–3696, 2017, doi: 10.3923/jeasci.2017.3692.3696.

[15] M. A. R. S. Al-Baghdadi, M. I. Roldán, J. Fernández-Reche, L. Valenzuela, A. Vidal, and E. Zarza, “ENERGY AND ENVIRONMENT FOUNDATION Engineering Applications of Computational Fluid Dynamics Chapter ** CFD MODELLING IN SOLAR THERMAL ENGINEERING,” pp. 1–38, 2015, [Online]. Available: www.IEEFoundation.org.

[16] H. Zang, M. Guo, Z. Wei, and G. Solar, “Determination of the optimal tilt angle of solar collectors for different climates of China,” Sustain., vol. 8, no. 7, pp. 1–16, 2016, doi: 10.3390/su8070654.

[17] S. Alsadi and Y. F. Nassar, “Correction of the ASHRAE clear-sky model parameters based on solar radiation measurements in the Arabic countries,” Int. J. Renew. Energy Technol. Res., vol. 5, no. 4, pp. 1–16, 2016, [Online]. Available: http://ijretr.org1.

[18] C. A. F. Ramos, A. N. Alcaso, and A. J. M. Cardoso, “Photovoltaic-thermal (PVT) technology: Review and case study,” IOP Conf. Ser. Earth Environ. Sci., vol. 354, no. 1, pp. 0–11, 2019, doi: 10.1088/1755-1315/354/1/012048.

[19] M. Y. Zulakmal et al., “Computational fluid dynamics analysis of thermoelectric generators performance under solar photovoltaic-thermal (PVT) system,” J. Adv. Res. Fluid Mech. Therm. Sci., vol. 56, no. 2, pp. 223–232, 2019.

[20] ABBAS, M. F. A., İbrahim, KOÇ., & ALJANABI, A. F. K. Modeling and Simulation to Investigate the Thermal Efficiency of a Parabolic Solar Trough Collector with Absorber Tube Inserted Twisted Tape System. AURUM Journal of Engineering Systems and Architecture, 2021, 5(1), 65-88.

[21] A. Mandal and M. K. Nigam, “Design And Development Of Solar PVT System,” Int. J. Eng. Res. Technol., vol. 1, no. 10, pp. 46–54, 2012.

[22] K. Naser and O. Ali, “Computational Design Optimization of the Solar Islands in the United Arab Emirates,” pp. 1–22.

[23] H. Chen, Y. Wang, Y. Ding, B. Cai, and J. Yang, “Numerical Analysis on the Performance of High Concentration Photovoltaic Systems Under the Nonuniform Energy Flow Density,” Front. Energy Res., vol. 9, no. July, pp. 1–11, 2021, doi: 10.3389/fenrg.2021.705801.

[24] Saghafifar, M., & Gadalla, M.. Thermo-economic analysis of air bottoming cycle hybridization using heliostat field collector: A comparative analysis. 2016, Energy, 112, 698-714.

[25] S. Abdul-Ganiyu, D. A. Quansah, E. W. Ramde, R. Seidu, and M. S. Adaramola, “Investigation of solar photovoltaic-thermal (PVT) and solar photovoltaic (PV) performance: A case study in Ghana,” Energies, vol. 13, no. 11, 2020, doi: 10.3390/en13112701.

[26] M. A. M. Rosli et al., “Simulation study of computational fluid dynamics on photovoltaic thermal water collector with different designs of absorber tube,” J. Adv. Res. Fluid Mech. Therm. Sci., vol. 52, no. 1, pp. 12–22, 2018.

[27] M. Hammami, S. Torretti, F. Grimaccia, and G. Grandi, “Thermal and performance analysis of a photovoltaic module with an integrated energy storage system,” Appl. Sci., vol. 7, no. 11, 2017, doi: 10.3390/app7111107.

[28] S. Misha, A. L. Abdullah, N. Tamaldin, M. A. M. Rosli, and F. A. Sachit, “Simulation CFD and experimental investigation of PVT water system under natural Malaysian weather conditions,” Energy Reports, vol. 6, pp. 28–44, 2020, doi: 10.1016/j.egyr.2019.11.162.

[29] S. Vaishnav, V. Kapadiya, R. Harish, and R. Mohan, “Design and analysis of energy-efficient solar panel cooling system using computational fluid dynamics,” IOP Conf. Ser. Mater. Sci. Eng., vol. 1128, no. 1, p. 012033, 2021, doi: 10.1088/1757-899x/1128/1/012033.

[30] J. Kim and Y. Nam, “Study on the cooling effect of attached fins on PV using CFD simulation,” Energies, vol. 12, no. 4, 2019, doi: 10.3390/en12040758.

[31] M. S. Rajagopal and M. Vedavyasa, “Thermal Management of Solar Power Pack using Computational Fluid Dynamics,” vol. 3, no. 17, pp. 1–10, 2015, [Online]. Available: https://scholar.google.com/citations?view_op=view_citation&hl=en&user=Ia0RnQMAAAAJ&pagesize=100&citation_for_view=Ia0RnQMAAAAJ:W7OEmFMy1HYC.

[32] M. Alobaid, B. Hughes, D. O’Connor, J. Calautit, and A. Heyes, “Improving thermal and electrical efficiency in photovoltaic thermal systems for sustainable cooling system integration,” J. Sustain. Dev. Energy, Water Environ. Syst., vol. 6, no. 2, pp. 305–322, 2018, doi: 10.13044/j.sdewes.d5.0187.

[33] N. Khordehgah, A. Żabnieńska-Góra, and H. Jouhara, “Energy performance analysis of a PV/T system coupled with domestic hot water system,” ChemEngineering, vol. 4, no. 2, pp. 1–14, 2020, doi: 10.3390/chemengineering4020022.

[34] A. M. Elbreki, A. F. Muftah, K. Sopian, H. Jarimi, A. Fazlizan, and A. Ibrahim, “Experimental and economic analysis of passive cooling PV module using fins and

planar reflector," Case Stud. Therm. Eng., vol. 23, no. December 2020, p. 100801, 2021, doi: 10.1016/j.csite.2020.100801.

[35] A. Sanz, "Systems Numercal simulation tools for PVT colectors - Task 60/Report Cl," p. 5, 2020, doi: 10.1777/ieashe-task 2020-06. [36] R. Senthil Kumr, N. Puja Priyadharshni, and E. Natarjan, "Experimntal and Computatinal Fluid Dynamics (CFD) Study of Glazed Three Dimnsional PVT Solar Panel with Air Cooling," Appl. Mech. vol. 787, no. Aug 2015, pp. 12-106, 2015, doi: 10.4028/www.seientfic.net/amm.787.102.

[37] Dirlcer, J., Juggurnth, D., Kays, A., Osowde, E. A., Simpson, M., Lecmpte, S., ... & Markids, C. N. (2019). Thermal energy proceses in direct steam generation solar systems: Boiling, condenstion and energy storage—A review. Frontirs in Energy Resarch, 6, 147.

[38] Leonard, M. D., MirhaPlids, E. E., & Michaelids, D N (2020). Energy storag needs for the substitutin of fosil fuel power plants with renewbles. Renewble Energy, 15, 91-92.

[39] Singh, R. (2021). Solar-city plans with large-scale energy storage: Metres to asses the ability to replace fosil-fuel based power. Sustainble Energy Technologes and Asessments, 44, 101065.

[40] Solanlci, S. C., Duby, S., & Tiwari, A. (2009). Indor simultion and testing of photovltaic thermal (PV/T) air colectrs. Applied energy, 86(1), 241-2428.

[41] Joslii, S. S., & Dhobl, A. S. (2018). Photovltaic-Thermal systems (PVT): Technology review and future trends. Renewble and Sustainble Energy Reviews, 92, 48-82.

[42] Hussain, M. T., & Mandi, E. J. (2018, May). Assesment of Solar Photovltaic Potental in Iraq. In Journal of Physics: Conference Series (Vol. 1032, No. 1, p. 012007). IOP Publishing.

[43] Al-Kayim, H. H., & Mohamad, S. T. (2019). Potental of renewble energy resorces with an emphasis on solar power in Iraq: An outlok Resorces, (1), 42.

[44] Khordehgh, N., Zabniaika-Gora, A., & Jouhar, H. (2020). Energy performnce analysis of a PV/T system copied with domestic hot water system. ChmEnginering, (2), 22.

[45] Abdul-Ganiyu, S., Qunsah, D. A., Ramd, E. W., Sidu, IL, & Adaramol, M. S. (2020). Investgation of solar photoltaic-thermal (PVT) and solar photovltaic (PV) performnce: A case study in Ghana. Eng, 13(1), 201.

[46] Kulkami, it S., Talnge, D. B., Dharm, A. A., & Mat, N. V. (2020). Developmnt and performnce analysis of solar photovltaic—thermal (PVT) system. Sadhana, (1), 1-5.

[47] Zang, H., Gu, M., Wi, Z., & Solar, G. (2016). Determnation of the optmal tilt angle of solar colectors for diferent climats of China. Sustainability, 8(7), 54.

[48] Misha, S., Abdulah, A. L., Tamaldin, N., Roth, M. A. M., & Sachit, F. A. (2020). Simulation CFD and experimntal investigtion of PVT water system under natural Malaysia weather condition. Energy Reports, 6, 8-44.

[49] Ghadiri, M., Sardrabadi, M., Pasndideh-fard, M., & Moghdam, A. J. (2015). Exprimental instigation of a PVT system performanc using nano ferofluids. Energy Conversion and Management, 13, 46-476.

[50] Duby, S., & Tay, A. A. (2013). Testing of different types of photovltaic-thrmal (PVT) modles with heat flow patern under tropical climatic condition. Energy for Sustinable Devlopment, 17(1), 1-12.

[51] He, R F., Zhng, M. R., & Hang, J. B. (2021). The dyamic effects of renwable-energy and fosil-fuel technlogical progres on metal consmption in the electric power industry. Resources Policy, 71, 101985.

[52] Shamandi, S. A., Rasoli Jazi, S., & Sharfdost, M. (2021). Determing the best lat of photovitaic systems in zero energy buldings using statstical inference aproach. Energy Equpment and Systems, 9(2), 107-116.

[53] Hamad, H. M., Mohamed, S. J., & Jabar, M. F. (2022). Optmization Of Tbrmal Modle Solar Photovltak Using CFDISimulation. In IOP Conference Series: Earth and Environmental Science (Vol. 961, No. 1, p. 012092). IOP Publishing.

[54] Temps, Ralph C., and K. L. Coulson. "Solar radiation incident upon slopes of different orientations." Solar energy 19.2 (1977): 179-184.

[55] Matuszko, Dorota. "Influence of the extent and genera of cloud cover on solar radiation intensity." International Journal of climatology 32.15 (2012): 2403-2414.

[56] Hinteregger, H. E. "Absolute intensity measurements in the extreme ultraviolet spectrum of solar radiation." Space Science Reviews 4.4 (1965): 461-497.

[57] Kimball, Herbert H. "Records of total solar radiation intensity and their relation to daylight intensity." Monthly weather review 52.10 (1924): 473-478.

[58] Shubbar, Ramiz M., Hassan H. Salman, and Dong-In Lee. "Characteristics of climate variation indices in Iraq using a statistical factor analysis." International Journal of Climatology 37.2 (2017): 918-927.